

WRN exonuclease imparts high fidelity on translesion synthesis by Y family DNA polymerases

Jung-Hoon Yoon, Karthi Sellamuthu, Louise Prakash, and Satya Prakash

Department of Biochemistry and Molecular Biology, University of Texas Medical Branch at Galveston, Galveston, Texas 77555, USA

Purified translesion synthesis (TLS) DNA polymerases (Pols) replicate through DNA lesions with a low fidelity; however, TLS operates in a predominantly error-free manner in normal human cells. To explain this incongruity, here we determine whether Y family Pols, which play an eminent role in replication through a diversity of DNA lesions, are incorporated into a multiprotein ensemble and whether the intrinsically high error rate of the TLS Pol is ameliorated by the components in the ensemble. To this end, we provide evidence for an indispensable role of Werner syndrome protein (WRN) and WRN-interacting protein 1 (WRNIP1) in Rev1-dependent TLS by Y family Pol η , Pol ι , or Pol κ and show that WRN, WRNIP1, and Rev1 assemble together with Y family Pols in response to DNA damage. Importantly, we identify a crucial role of WRN's 3' \rightarrow 5' exonuclease activity in imparting high fidelity on TLS by Y family Pols in human cells, as the Y family Pols that accomplish TLS in an error-free manner manifest high mutagenicity in the absence of WRN's exonuclease function. Thus, by enforcing high fidelity on TLS Pols, TLS mechanisms have been adapted to safeguard against genome instability and tumorigenesis.

[*Keywords:* DNA repair; DNA lesions; UV damage; Werner syndrome protein WRN; Y family DNA polymerases; fidelity of translesion synthesis]

Supplemental material is available for this article.

Received December 4, 2023; revised version accepted February 26, 2024.

Translesion synthesis (TLS) polymerases (Pols) promote replication through DNA lesions. Biochemical, structural, and genetic studies have indicated a high degree of specificity for the types of DNA lesions through which TLS Pols can replicate. Thus, among the Y family Pols, which play a paramount role in replication of damaged DNA, the unique ability of Pol η to accommodate the two covalently linked pyrimidines of a cyclobutane pyrimidine dimer (CPD) in its active site allows it to replicate through the CPD by forming a Watson–Crick (W-C) base pair with the incoming nucleotide (Johnson et al. 1999, 2005; Masutani et al. 1999; Biertümpfel et al. 2010; Silverstein et al. 2010). In striking contrast, the proficiency of Pol ι in pushing a template A or G purine into a *syn* conformation and in forming a Hoogsteen base pair with the incoming nucleotide enables it to insert nucleotides opposite DNA adducts that impair W-C base pairing (Nair et al. 2004, 2005, 2006a,b). Altogether, the active sites of TLS Pols are adapted for accommodating different types of DNA lesions and are specialized either for inserting a nucleotide opposite the lesion site or for performing extension of synthesis from the nucleotide inserted oppo-

site the DNA lesion by another Pol (Johnson et al. 2000a; Prakash and Prakash 2002; Prakash et al. 2005).

The high specificity of TLS Pols for replicating past particular type(s) of DNA lesions is accompanied by an extremely low fidelity. This is because, unlike the high-fidelity replicative Pols that have a constrained active site and possess a 3' \rightarrow 5' proofreading exonuclease activity, TLS Pols have a more open active site and lack proofreading activity. Despite the low fidelity of purified TLS Pols, however, TLS that occurs during replication in normal human cells (not derived from cancers) operates in a predominantly error-free manner. For example, whereas purified human Pol η misincorporates nucleotides opposite the 3'T or 5'T of a *cis-syn* TT dimer with a very high frequency of $\sim 10^{-2}$ (Johnson et al. 2000b), Pol η conducts error-free TLS through CPDs in human or mouse cells (Yoon et al. 2009, 2019b). Even more remarkably, despite the fact that purified Pol ι misincorporates a C opposite the W-C-impairing adduct 1,N⁶-ethenodeoxyadenosine (ϵ Ad) (which is formed by interaction of DNA with aldehydes

Corresponding author: saprakas@utmb.edu

Article published online ahead of print. Article and publication date are online at <http://www.genesdev.org/cgi/doi/10.1101/gad.351410.123>.

© 2024 Yoon et al. This article is distributed exclusively by Cold Spring Harbor Laboratory Press for the first six months after the full-issue publication date (see <http://genesdev.cshlp.org/site/misc/terms.xhtml>). After six months, it is available under a Creative Commons License (Attribution-NonCommercial 4.0 International), as described at <http://creativecommons.org/licenses/by-nc/4.0/>.

derived from lipid peroxidation in cell membranes) with only an approximately threefold reduction in catalytic efficiency than that for the incorporation of the correct nucleotide T (Nair et al. 2006a), it conducts error-free TLS opposite ϵ A in human cells (Yoon et al. 2019a).

To explain the contradiction that intrinsically error-prone TLS Pols perform predominantly error-free TLS in human cells, we have previously suggested that TLS Pols in human cells are incorporated into multiprotein ensembles in which the error-proneness of the TLS Pol is attenuated to a large degree by the components in the ensemble (Yoon et al. 2009, 2010a, 2014, 2017, 2018, 2019a, 2021b; Conde et al. 2015). The identification of Rev1 as an indispensable scaffolding component for each of the Y family Pols suggested that the other proteins that function together with Pol η , Pol ι , or Pol κ might be identical, brought together by Rev1's scaffolding role (Yoon et al. 2015). In accordance with this, in this study we identified Werner syndrome protein (WRN) and WRN-interacting protein 1 (WRNIP1) as the additional components shared among Y family Pols.

WRN is a member of the RecQ family of DNA helicases. It contains a RecQ-type helicase domain in the central region and an exonuclease domain in the N-terminal region (Chu and Hickson 2009), and purified WRN exhibits a 3' \rightarrow 5' DNA helicase activity (Gray et al. 1997; Shen et al. 1998) and a 3' \rightarrow 5' DNA exonuclease activity that can efficiently remove 3'-terminal mispairs (Huang et al. 1998, 2000; Kamath-Loeb et al. 1998; Choudhary et al. 2004; Perry et al. 2006). Mutations in *WRN* are associated with Werner syndrome (WS), characterized by premature aging and a high predisposition for cancers (Goto et al. 2013; Lauper et al. 2013; Oshima et al. 2017). Almost all the large numbers of mutations in *WRN* that have been identified in Werner's patients are nonsense, splicing, or insertion/deletion mutations, and all of these mutations result in disruption of the open reading frame and lead to loss of WRN function by destabilizing the protein or by the failure of WRN to localize in the nucleus (Huang et al. 2006; Fu et al. 2017; Yokote et al. 2017; Lebel and Monnat 2018).

WRNIP1 was initially identified as a protein that physically interacts with WRN (Kawabe et al. 2001). WRNIP1 has Walker type A and Walker type B ATPase domains and exhibits a DNA-dependent ATPase activity; at the N terminus, WRNIP1 has a ubiquitin binding zinc finger (UBZ) domain (Kawabe et al. 2001; Tsurimoto et al. 2005).

Here we show that WRN and WRNIP1 are specifically required for TLS mediated by Y family Pol η , Pol ι , or Pol κ . Furthermore, we provide evidence that WRN and WRNIP1, along with Rev1, assemble together with Y family Pols in response to DNA damage, and most importantly, we identified a crucial role for WRN's 3' \rightarrow 5' exonuclease activity in imparting high fidelity on TLS by Y family Pols in human and mouse cells. The adaptation of Y family Pols to perform predominantly error-free TLS in human cells raises the strong possibility that the fidelity of other highly error-prone TLS Pols would be similarly modulated by the other protein factors. Thus, by promoting predominantly error-free replication

through DNA lesions, TLS mechanisms would provide an effective barrier against genome instability and tumorigenesis rather than contribute to it—a deeply set percept.

Results

Indispensability of WRN for TLS by Y family Pols opposite UV lesions

To analyze the genetic control of TLS in human cells, we used a duplex plasmid in which bidirectional replication initiates from an origin of replication, and the frequency of TLS through the DNA lesion, carried on the template for leading or lagging strand replication, is determined by the frequency of blue colonies among Kan⁺ colonies (Yoon et al. 2009, 2010b). Altogether, our evidence in previous studies (Yoon et al. 2012, 2019b) as well as in this study affirms the conclusion that the TLS mechanisms inferred from this plasmid system reflect those that operate during genomic replication.

We have shown previously that TLS through CPDs is promoted by a Pol η -dependent error-free pathway or via an alternative Pol θ -dependent error-prone pathway (Yoon et al. 2019b). Because of the proficient ability of Pol η to insert nucleotides opposite both the 3'T and 5'T of a *cis-syn* TT dimer and to subsequently extend synthesis, Pol η alone performs TLS through the dimer. In the Pol θ pathway, however, following nucleotide insertion opposite the 3' pyrimidine of the dimer by Pol θ (Yoon et al. 2019b), Pol κ or Pol ζ would extend synthesis from the nucleotide inserted by Pol θ (Supplemental Fig. S1A; Johnson et al. 2000a; Washington et al. 2002).

In Table 1, we provide evidence for WRN's role in TLS opposite a *cis-syn* TT dimer or a (6-4) TT photoproduct in conjunction with Y family Pols. In nucleotide excision repair (NER)-defective XPA human fibroblasts (HFs), TLS opposite a *cis-syn* TT dimer present on the leading strand template of the plasmid occurs with a frequency of ~40%, and in cells depleted for WRN (Supplemental Fig. S2A), TLS is reduced to ~13% (Table 1). In cells depleted for Rev1 alone or codepleted for Rev1 and WRN, TLS occurs at the same frequency as in WRN-depleted cells. This observed epistasis indicates a role of WRN in the Rev1-dependent pathway for TLS opposite the TT dimer. Since Rev1 is required for TLS dependent on all Y family Pols (Yoon et al. 2015), we next verified that WRN depletion exhibits epistasis with TLS by the other Y family Pols. TLS in cells depleted for Pol η alone occurs at a frequency of ~19%, and TLS in cells codepleted for WRN and Pol η declines to the same level as in cells depleted for WRN alone, consistent with epistasis of WRN over Pol η (Table 1). Because of the requirement of WRN for TLS by Pol η , or by Pol κ in the Pol θ /Pol κ pathway (Supplemental Fig. S1A), only the Pol θ /Pol ζ pathway would be functional in WRN-depleted cells; hence, we expected that TLS would be annulled in cells codepleted for WRN with Pol θ or Pol ζ . The drastic reduction in TLS frequency to ~4% in cells codepleted for WRN with Pol θ or with the Rev3 catalytic subunit of Pol ζ confirms a role for WRN in TLS in

Table 1. Requirement of WRN and WRNIP1 for Y family Pol-dependent TLS opposite a *cis-syn* TT dimer or a (6-4) TT photoproduct carried on the leading strand DNA template in NER-defective XPA HFs

DNA lesion	siRNA	Number of <i>Kan</i> ⁺ colonies	Number of blue colonies among <i>Kan</i> ⁺	TLS (%)
<i>cis-syn</i> TT dimer	NC	408	164	40.2
	WRN	385	52	13.5
	WRNIP1	407	54	13.3
	Rev1	425	58	13.6
	Pol η	416	80	19.2
	Pol θ	372	69	18.5
	Rev3	368	104	28.3
	WRN + Rev1	409	51	12.5
	WRN + Pol η	346	48	13.9
	WRN + Pol θ	369	15	4.1
	WRN + Rev3	374	18	4.8
	WRNIP1 + WRN	384	50	13.0
	WRNIP1 + Rev1	408	54	13.2
	WRNIP1 + Rev3	357	12	3.4
(6-4) TT photoproduct	NC	436	148	33.9
	WRN	412	56	13.6
	WRNIP1	376	49	13.0
	Rev1	394	54	14.2
	Pol θ	368	58	15.8
	Rev3	406	58	14.3
	Rev7	443	62	14.0
	WRN + Rev1	328	48	14.6
	WRN + Pol θ	433	60	13.9
	WRN + Rev3	415	21	5.1
	WRN + Rev7	392	18	4.6
	WRNIP1 + WRN	412	52	12.6
	WRNIP1 + Rev1	364	47	12.9
	WRNIP1 + Rev3	323	13	4.0

pathways that act independently of the Pol θ /Pol ζ pathway (Table 1).

To further add to the evidence for WRN's requirement for TLS opposite a *cis-syn* TT dimer by Y family Pols, we analyzed the effects of depletions of Y family Pols on TLS in WRN^{-/-} HFs. As shown in Supplemental Table S1, whereas TLS in WRN^{+/+} HFs occurs at a frequency of ~25%, the TLS frequency declines to ~10% in WRN-depleted cells. In WRN^{-/-} HFs treated with control (NC) siRNA, TLS occurs at ~8%, and the TLS frequency remains nearly the same in WRN^{-/-} cells depleted for either Rev1, Pol η , or Pol κ . These epistatic effects of WRN add further support for a role for WRN in Rev1-dependent TLS by Pol η or Pol κ . Furthermore, the large reduction in TLS frequency (to ~2%) in WRN^{-/-} cells depleted for either Pol θ , Rev3, or Rev7 aligns with WRN's role in TLS pathways that operate independently of Pol θ and Pol ζ .

TLS through a (6-4) TT photoproduct occurs via error-prone pathways dependent on Pol η /Pol θ or Pol ι /Pol θ and an error-free pathway dependent on Pol λ /Pol ζ (Supplemental Fig. S1B; Yoon et al. 2010b, 2019b, 2021a). In the Pol η /Pol θ or Pol ι /Pol θ pathways, following nucleotide in-

sertion opposite the 3'T of the photoproduct by Pol η or Pol ι (Johnson et al. 2000a, 2001), Pol θ would extend synthesis (Yoon et al. 2019b). In the Pol λ /Pol ζ pathway, following nucleotide insertion by Pol λ (Yoon et al. 2021a), Pol ζ would extend synthesis (Supplemental Fig. S1B; Johnson et al. 2000a). The requirement of WRN for TLS by Y family Pols implies that Pol η /Pol θ - or Pol ι /Pol θ -dependent TLS would be inhibited in WRN-deficient cells and that Pol ζ -dependent TLS would remain active. In addition, because of the indispensability of Rev1 for TLS by Pol η or Pol ι , TLS by these Pols would be inhibited in Rev1-deficient cells. As shown in Table 1, TLS occurs at a frequency of ~34% in control (NC) cells, whereas the TLS frequency is reduced to a similar level (~14%) in cells depleted for WRN or Rev1 or codepleted for WRN and Rev1, implicating a role of WRN in Rev1-dependent TLS by Pol η or Pol ι opposite a (6-4) TT photoproduct. However, because of the requirement of Pol θ for extension of synthesis pursuant to nucleotide insertion by Pol η or Pol ι , a similar reduction in TLS frequency occurs in cells depleted for WRN or Pol θ alone or codepleted for both WRN and Pol θ (Table 1). As expected from the role of WRN in TLS via

pathways that require Y family Pols, codepletion of WRN with Rev3 or Rev7 leads to a large reduction in TLS frequency to ~5% (Table 1). We additionally confirmed these results in WRN^{-/-} HF (Supplemental Table S1).

Furthermore, we determined whether WRN's helicase activity was required for TLS. However, WRN's helicase activity is not required for TLS, as the TLS frequency opposite a *cis-syn* TT dimer or a (6-4) TT photoproduct in WRN^{-/-} HF expressing ATPase/helicase-defective K577A WRN (Newman et al. 2021) remains the same as in cells expressing WT WRN (Supplemental Table S2).

Role of WRN in predominantly error-free TLS opposite UV lesions

Next, we analyzed the effect of WRN deficiency on UV-induced mutations resulting from TLS opposite CPDs—the preponderant UV lesion (80%) (Pfeifer 1997; Yoon et al. 2000; You et al. 2001)—formed at TT, TC, CT, and CC dipyrimidine sites in the *cII* gene, which has been integrated into the genome of big blue mouse embryonic fibroblasts (BBMEFs). The spectrum of mutations induced by UV and other DNA-damaging agents in the *cII* gene resembles that determined from sequence analyses of endogenous chromosomal genes and from whole-genome sequence analyses (You and Pfeifer 2001; You et al. 2001; Besaratinia and Pfeifer 2006; Alexandrov et al. 2013; Mar-

tincorena et al. 2015; Yoon et al. 2021a). To examine UV mutations that result specifically from TLS opposite CPDs, (6-4) PPs were selectively removed by expressing a (6-4) PP photolyase gene in the BBMEF cell line and treatment with photoreactivating light (You et al. 2001). In this cell line, spontaneous mutations occurred at a frequency of $\sim 15 \times 10^{-5}$, and the frequency remained about the same in WRN-depleted cells (Table 2). In UV-irradiated (5 J/m^2) WT cells exposed to photoreactivating light, the mutation frequency resulting from TLS through CPDs rose to $\sim 47 \times 10^{-5}$. In Pol η -depleted cells, the mutation frequency rose to $\sim 90 \times 10^{-5}$, whereas in Polk- or Rev3-depleted cells, the mutation frequency declined to $\sim 30 \times 10^{-5}$ (Table 2). These data are consistent with the respective roles of Pol η in error-free TLS and of Polk or Pol ζ in error-prone TLS (Yoon et al. 2009). In BBMEFs depleted for WRN, UV-induced mutations opposite CPDs occurred at a frequency of $\sim 70 \times 10^{-5}$, nearly similar to the frequency in Rev1-depleted cells (Table 2). Our results showing that in cells codepleted for WRN with either Pol η , Polk, or Rev1, UV-induced mutations occur at the same frequency ($\sim 70 \times 10^{-5}$) as in cells depleted for WRN alone (Table 2) implicate that WRN, similar to Rev1, is involved in error-free TLS by Pol η and in error-prone TLS by Polk (Supplemental Fig. S1A). Furthermore, the evidence that in cells codepleted for WRN with Rev3, the frequency of UV-induced mutations declines to near-spontaneous levels

Table 2. Epistatic effects of WRN on Y family Pols for UV-induced mutations in the *cII* gene resulting from TLS through CPDs or (6-4) PPs

Photolyase	siRNA	UV ^a	Photoreactivation ^b	Mutation frequency ^c ($\times 10^{-5}$)
(6-4) PP	NC	–	+	15.4 ± 0.6
	WRN	–	+	16.2 ± 0.7
	NC	+	+	47.5 ± 1.4
	Pol η	+	+	89.4 ± 1.5
	Polk	+	+	31.0 ± 0.8
	Rev3	+	+	29.5 ± 0.6
	WRN	+	+	70.5 ± 1.3
	Rev1	+	+	75.0 ± 2.1
	Pol η + WRN	+	+	68.8 ± 1.3
	Polk + WRN	+	+	71.5 ± 1.7
	Rev1 + WRN	+	+	70.2 ± 1.3
	Rev3 + WRN	+	+	19.4 ± 1.1
	CPD	NC	–	+
WRN		–	+	15.3 ± 0.6
NC		+	+	26.9 ± 1.2
WRN		+	+	17.3 ± 0.8
Rev1		+	+	17.8 ± 0.9
Rev3		+	+	40.5 ± 1.2
Rev1 + WRN		+	+	18.3 ± 1.3
Rev3 + WRN		+	+	18.9 ± 1.4

^a5 J/m² of UVC (254-nm) light.

^bPhotoreactivation with UVA (360-nm) light for 3 h.

^cData are represented as mean ± SEM. Mean mutation frequencies and standard error of the mean were calculated from four independent experiments.

($\sim 19 \times 10^{-5}$) (Table 2) affirms the conclusion that in WRN-deficient cells, only the error-prone Pol θ /Pol ζ pathway remains operational (Supplemental Fig. S1A).

To examine UV mutations resulting specifically from TLS opposite (6-4) PPs formed at the various dipyrimidine sites, the CPDs were selectively removed from the genome by expressing a CPD photolyase gene in BBMEFs (You et al. 2001). In this cell line, spontaneous mutations occurred at a frequency of $\sim 17 \times 10^{-5}$ and were not significantly affected by WRN depletion (Table 2). In UV-irradiated cells (5 J/m^2) exposed to photoreactivating light to activate CPD photolyase, mutation frequency rose to $\sim 27 \times 10^{-5}$. Depletion of WRN or Rev1 alone or codepletion of WRN with Rev1 reduced UV-induced mutation frequency to a level similar to that in unirradiated cells (Table 2), consistent with their requirement for error-prone TLS by the Pol η /Pol θ or Pol ι /Pol θ pathway (Supplemental Fig. S1B). Depletion of Rev3 raised mutation frequency to $\sim 40 \times 10^{-5}$, and codepletion of Rev3 with WRN reduced UV-induced mutation frequency nearly similarly to that in unirradiated cells (Table 2). Altogether, these results confirm WRN's involvement in Rev1-dependent error-prone TLS by Pol η or Pol ι in the Pol η /Pol θ or Pol ι /Pol θ pathway that operates independently of Pol ζ -dependent error-free TLS opposite (6-4) PPs (Supplemental Fig. S1B).

UV-induced C > T and CC > TT signature mutations resulting from mutagenic TLS through CPDs accumulate in the *cII* gene at hotspots located at 11 dipyrimidine sequences (#1–#11) in WT cells. In WRN-depleted cells, mutational hotspots at positions #4, #5, #7, and #8 remain, while the mutational hotspots at other positions are ablated (Supplemental Fig. S3A). We have shown previously that error-prone TLS through CPDs by Pol κ versus Pol ζ generates different spectra of hotspot mutations (Yoon et al. 2009), and consistent with the requirement of WRN for error-prone TLS by Pol κ (Supplemental Fig. S1A), the spectrum of hotspot mutations generated by WRN depletion is nearly identical to that caused by Pol κ depletion (Yoon et al. 2009). In WT cells, TLS through (6-4) PPs in the *cII* gene generates mutational hotspots at positions #1–#5 (Yoon et al. 2010b, 2021a). Consistent with the requirement of WRN for error-prone TLS by the Pol η - and Pol ι -dependent pathways, these mutational hotspots are absent in WRN-depleted cells (Supplemental Fig. S3B). Also, as expected from the similar requirement of WRN and Rev1 for TLS by Y family PPs opposite UV lesions, the pattern of hotspot mutations resulting from TLS through CPDs or (6-4) PPs in WRN-deficient cells resembles that in Rev1-deficient cells (Yoon et al. 2015).

WRN promotes replication fork progression through UV lesions in conjunction with Y family PPs

The requirement of WRN for TLS by Y family PPs opposite UV lesions implicated a crucial role for WRN in the replication of UV-damaged DNA. To verify this, we monitored replication fork (RF) progression on single DNA fibers. siRNA-treated HF cells were pulse-labeled with iododeoxyuridine (IdU) for 20 min and then UV-irradiated at 10 J/m^2 , followed by labeling with chlorodeoxyuridine (CldU) for 20

min. In undamaged cells, WRN depletion conferred no significant reduction in RF progression compared with control (NC) cells (Fig. 1A). In UV-irradiated cells, however, WRN depletion reduced RF progression by $\sim 45\%$ compared with that in control siRNA-treated HF cells, and a similar reduction occurred in Rev1-depleted HF cells (Fig. 1B).

Next, we examined RF progression in WRN $^{-/-}$ HF cells. RF progression was not significantly affected in unirradiated WRN $^{-/-}$ HF cells depleted or not for TLS PPs (Fig. 1C), and in UV-irradiated WRN $^{-/-}$ HF cells, RF progression was reduced by $>40\%$ compared with that in WT HF cells (Fig. 1D). To confirm the epistatic relationships of WRN with Rev1 and the various TLS PPs, we analyzed the effects of their siRNA depletion on RF progression in UV-irradiated WRN $^{-/-}$ HF cells (Fig. 1D). The lack of any effect of Rev1 or Pol η depletion on RF progression in WRN $^{-/-}$ HF cells concurs with WRN's role in promoting replication through UV lesions in conjunction with Y family PPs; in contrast, the reduction in RF progression in Pol θ - or Rev3-depleted WRN $^{-/-}$ HF cells (Fig. 1D) conforms with WRN's role in promoting replication through CPDs via pathways that operate independently of the Pol θ /Pol ζ pathway (Supplemental Fig. S1A).

Requirement of WRNIP1 for WRN-dependent TLS through UV lesions

To demonstrate WRNIP1's role in TLS in conjunction with WRN, we first analyzed the effects of WRNIP1 depletion (Supplemental Fig. S2C) on TLS through UV lesions in XPA HF cells and in WRN $^{-/-}$ HF cells. As shown in Table 1, in XPA HF cells depleted for WRNIP1, TLS opposite a *cis-syn* TT dimer was reduced to the same level ($\sim 13\%$) as in WRN- or Rev1-depleted cells, and TLS frequency remained the same in cells codepleted for WRNIP1 together with WRN or Rev1. The epistasis of WRNIP1 with WRN and Rev1 concurs with WRNIP1's role in TLS in conjunction with WRN and Rev1 (Table 1); additionally, we confirmed epistasis of WRNIP1 with WRN for TLS opposite a *cis-syn* TT dimer in WRN $^{-/-}$ HF cells (Supplemental Table S1). Furthermore, the large reduction in TLS frequency in cells codepleted for WRNIP1 and Rev3 (Table 1) conforms with WRNIP1's role in Pol ζ -independent TLS pathways (Supplemental Fig. S1A).

In XPA HF cells depleted for WRNIP1, TLS opposite a (6-4) TT PP occurred at the same frequency ($\sim 13\%$) as in cells depleted for WRN or Rev1 or codepleted for WRNIP1 together with WRN or Rev1, and TLS frequency declined to $\sim 4\%$ in cells codepleted for WRNIP1 and Rev3 (Table 1). These results concur with a role of WRNIP1 in Rev1/WRN-dependent TLS through (6-4) PPs that operates independently of Pol ζ -mediated TLS. We also affirmed the epistasis of WRNIP1 with WRN for TLS opposite a (6-4) TT PP in WRN $^{-/-}$ HF cells (Supplemental Table S1).

WRNIP1 promotes replication fork progression through UV lesions in conjunction with WRN

The requirement of WRNIP1 for WRN-dependent TLS through UV lesions implicates that, similar to WRN, WRNIP1 would affect RF progression through UV lesions.

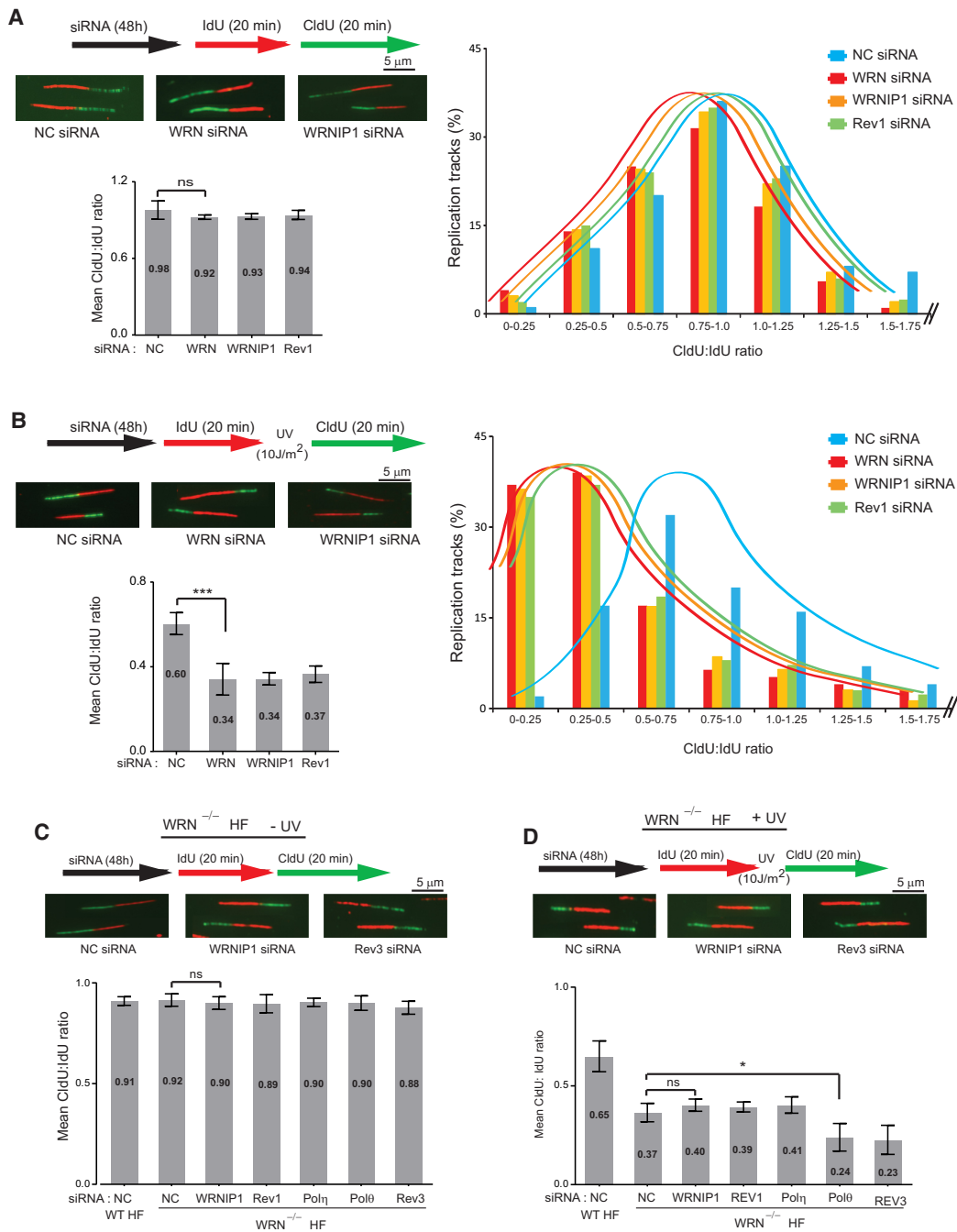


Figure 1. Requirement of WRN for replication through UV lesions in conjunction with WRNIP1, Rev1, and Y family Pols. (A) RF progression in unirradiated WT HF cells depleted for WRN, WRNIP1, or Rev1. (B) RF progression in UV-irradiated WT HF cells depleted for WRN, WRNIP1, or Rev1. (C) RF progression in unirradiated WRN^{-/-} HF cells depleted for WRNIP1 or TLS Pols. (D) RF progression in UV-irradiated WRN^{-/-} HF cells depleted for WRNIP1 or TLS Pols. In A–D, quantitative determination of RF progression (mean CldU:IdU ratio) was based on ~400 DNA fibers analyzed from four independent experiments. Error bars indicate the SD. *P*-values were derived using Student’s two-tailed *t*-test. (ns) Not significant, (*) *P* < 0.05, (***) *P* < 0.001.

Our results showing that in UV-irradiated HF cells, WRNIP1 depletion causes the same high level of reduction in RF progression as that conferred by WRN or Rev1 depletion (Fig. 1B), and that WRNIP1 depletion causes no further reduction in RF progression in UV-irradiated WRN^{-/-} HF cells (Fig. 1D) are consistent with the role of WRNIP1 in pro-

moting RF progression through UV lesions in conjunction with WRN and Rev1.

As expected from the role of WRNIP1 in WRN/Rev1-dependent replication through UV lesions, UV survival is reduced to the same level in WRNIP1-depleted HF cells as in WRN- or Rev1-depleted HF cells (Supplemental Fig. S4A),

and consistent with their epistatic relationship, UV survival of WRN^{-/-} HFs is not affected by depletion of WRNIP1 or Rev1 (Supplemental Fig. S4B).

UV-induced assembly of Y family Pols with WRN, WRNIP1, and Rev1

We have previously shown that Rev1 is required for the UV-induced assembly of Polη, Polι, or Polκ into replication foci and, conversely, that these Pols affect the assembly of Rev1 into foci (Yoon et al. 2015). Based on these results, we suggested that via its scaffolding role, Rev1 would promote the assembly of the same protein components in the respective multiprotein ensembles of each of these Pols (Yoon et al. 2015). Our evidence that WRN and WRNIP1 function together with Rev1 in TLS by Y family Pols strongly implicate that WRN and WRNIP1 are the additional components that assemble together with Y family Pols. To ascertain this, we analyzed the effects of WRN and WRNIP1 depletion on the accumulation of Rev1, Polη, Polι, or Polκ in UV-induced replication foci to determine whether their accumulation depends on one another.

Whereas ~14% of unirradiated cells contain WRN foci, UV damage induces WRN foci in >50% of cells (Fig. 2A). Our results that the UV-induced increase in WRN foci does not occur in Rev1- or WRNIP1-depleted cells indicate the requirement of Rev1 and WRNIP1 for WRN's assembly into foci (Fig. 2A); conversely, the ablation of UV-induced WRNIP1 foci in WRN- or Rev1-depleted cells implicate the requirement of WRN and Rev1 for WRNIP1 assembly into foci (Fig. 2B). Furthermore, the annulment of UV-induced Rev1 foci in WRN- or WRNIP1-depleted cells (Fig. 2C) conforms with the requirement of WRN and WRNIP1 for Rev1's assembly into foci (Fig. 2C). The requirement of WRN as well as WRNIP1 for the UV-induced assembly of Rev1 into foci (Fig. 2C) and the requirement of Rev1 for the UV-induced assembly of Y family Pols into foci (Yoon et al. 2015) implicate that WRN and WRNIP1 would be similarly required for the UV-induced assembly of Y family Pols; accordingly, we found that the UV-induced increase in Polη foci is abrogated in WRN- or WRNIP1-depleted cells (Fig. 2D). Similarly, a UV-induced increase in Polκ or Polι foci does not occur in WRN- or WRNIP1-depleted cells (Supplemental Fig. S5A, B). Additionally, as expected from the lack of WRN or WRNIP1 involvement in the Polζ-dependent TLS pathway opposite UV lesions, their depletion had no effect on the UV-induced assembly of the Rev7 subunit of Polζ into foci (Supplemental Fig. S5C).

We also determined whether in chromatin extracts from UV-irradiated HFs, Polη (which plays a predominant role in the replication of UV-damaged DNA) coimmunoprecipitates with Rev1, WRN, and WRNIP1. For these experiments, HFs stably expressing FLAG-Rev1 were UV-irradiated, chromatin extracts were prepared, and proteins bound to FLAG agarose beads were eluted. In chromatin extracts from UV-irradiated cells, Polη coimmunoprecipitated with Rev1, WRN, and WRNIP1, but in extracts from unirradiated cells, Polη failed to coimmunoprecipitate

with any of these proteins (Fig. 2E). Thus, Polη assembles with Rev1, WRNIP1, and WRN in response to UV damage.

Additionally, we verified the dependency of WRN, WRNIP1, or Rev1 on one another for localization into foci induced by treatment with cisplatin and their requirement for accumulation of Y family Pols into cisplatin-induced foci. In normal human cells, TLS through cisplatin intrastrand cross-links is promoted by Polη- or Polι-dependent pathways, both of which require Rev1 (Yoon et al. 2021b). Similar to what has been seen for UV lesions, the accumulation of WRN or WRNIP1 in cisplatin-induced foci depends on Rev1, and the accumulation of Rev1 in foci depends on WRN and WRNIP1. Moreover, the accumulation of Polη or Polι in cisplatin-induced foci depends on WRN, WRNIP1, and Rev1 (Supplemental Fig. S6).

Requirement of WRN and WRNIP1 for TLS by Y family Pols opposite other DNA lesions

To establish that the requirement of WRN and WRNIP1 for TLS by Y family Pols extends to other DNA lesions, we analyzed their role in TLS opposite thymine glycol (Tg) and 1,N⁶-ethenodeoxyadenosine (εdA). Tg is generated from the reaction of thymine with hydroxyl radicals resulting from aerobic respiration and from exposure to chemical oxidants or ionizing radiation, and TLS through this lesion is performed by Polκ/Polζ- or Polθ-dependent pathways (Supplemental Fig. S1C; Yoon et al. 2010a, 2014). As shown in Supplemental Table S3, in WT HFs, TLS opposite Tg occurs at a frequency of ~25%, and WRN or WRNIP1 depletion reduces TLS frequency to ~12%. In WRN^{-/-} HFs, TLS opposite Tg occurs at a frequency of ~13%, and this frequency remains the same in WRN^{-/-} HFs depleted for WRNIP1, Rev1, Polκ, Rev3, or Rev7. However, TLS frequency is reduced to ~4% in WRN^{-/-} HFs depleted for Polθ. The epistasis of WRN with WRNIP1, Rev1, and Polκ is congruent with the requirement of these proteins for TLS by Polκ. The epistasis of WRN with Rev3 or Rev7 derives from the role of Polζ in the same pathway as Polκ. In contrast, the drastic reduction in TLS frequency in WRN^{-/-} cells depleted for Polθ excludes WRN's role in the alternative Polθ pathway.

εdA is formed in DNA through interaction with aldehydes derived from lipid peroxidation, a normal chain reaction process that initiates from the oxidation of polyunsaturated fatty acids in cell membranes and results in the formation of a variety of highly reactive aldehydes. TLS opposite εdA is performed by two major Polι/Polζ- and Polθ-dependent pathways and by a minor pathway that requires Rev1 polymerase activity (Supplemental Fig. S1D; Yoon et al. 2019a). As shown in Supplemental Table S3, TLS opposite εdA in WT HFs occurs at a frequency of ~23%, and this frequency is reduced to ~11% in WRN- or WRNIP1-depleted cells. In WRN^{-/-} HFs, TLS opposite εdA occurs at a frequency of ~8%, and TLS frequency remains the same in WRN^{-/-} HFs depleted for WRNIP1, Rev1, Polι, or Rev3 (Polζ) (Supplemental Table S3), congruent with a role for WRN and WRNIP1 in TLS in conjunction with Rev1 and Polι in the Polι/Polζ pathway. The large

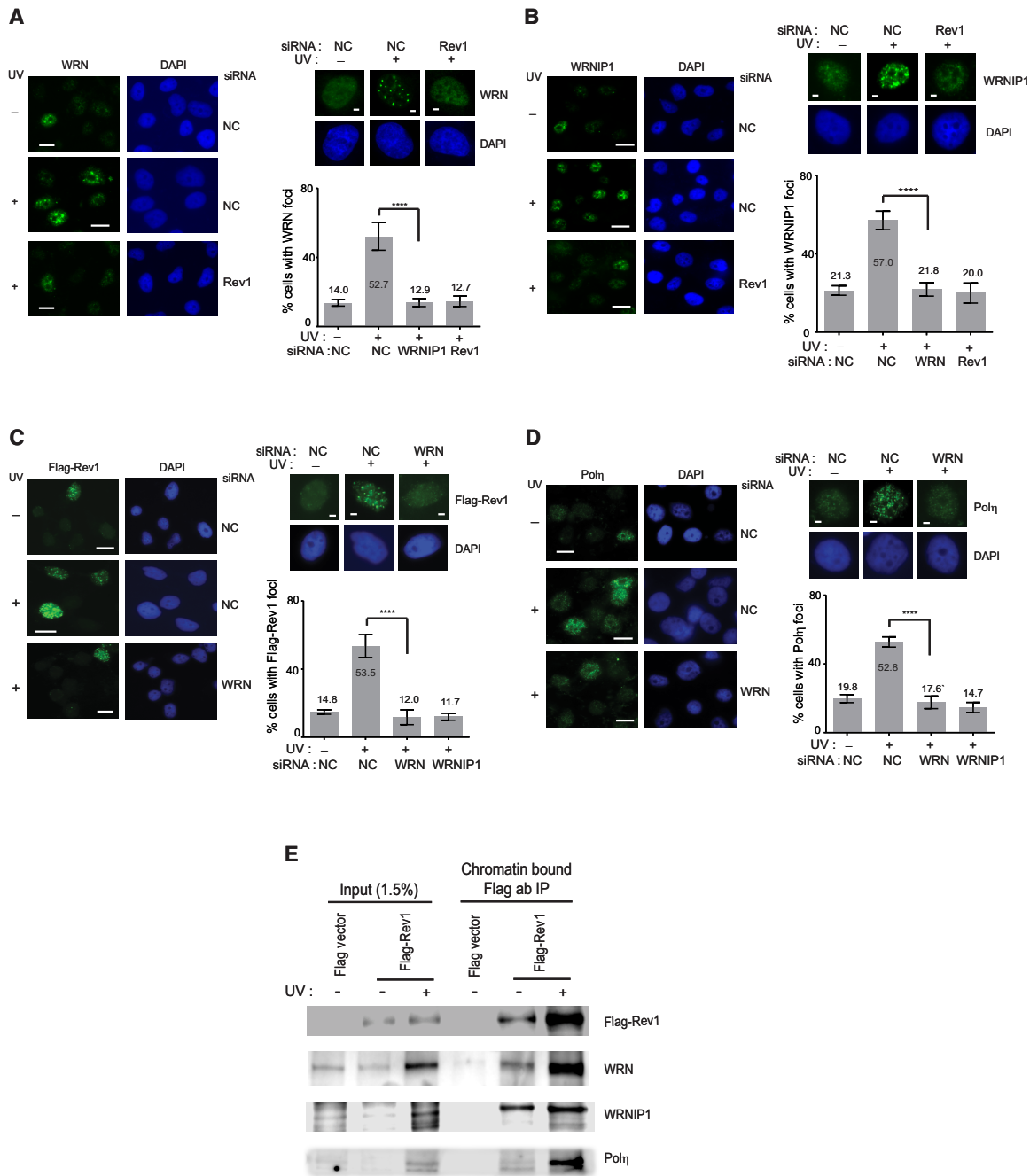


Figure 2. UV-induced assembly of WRN, WRNIP1, and Rev1 with Y family Pols. (A) Requirement of WRNIP1 and Rev1 for the assembly of WRN into UV-induced foci. (B) Requirement of WRN and Rev1 for the assembly of WRNIP1 into UV-induced foci. (C,D) Requirement of WRN and WRNIP1 for the assembly of Rev1 (C) and Polη (D) into UV-induced foci. In A–D, error bars indicate the SD. *P*-values were derived using Student’s two tailed *t*-test. (****) *P* < 0.0001. For each analysis, ~200–300 cells were analyzed. Scale bars: A, left, 10 μm; A, right, 2 μm. (E) Coimmunoprecipitation (co-IP) of FLAG-Rev1 with WRN, WRNIP1, and Polη in chromatin fractions from UV-irradiated cells. GM00637 HF cells expressing FLAG-Rev1 were UV-irradiated and incubated for 4 h. Chromatin extracts from unirradiated and UV-irradiated cells were immunoprecipitated with FLAG M2 agarose (Sigma). Co-IPs of FLAG-Rev1 with WRN, WRNIP1, and Polη were determined by Western blot analysis.

reduction in TLS frequency in WRN^{-/-} HF cells depleted for Polθ aligns with WRN’s role in TLS independent of Polθ (Supplemental Table S3).

TLS analyses opposite the Tg and εdA lesions clearly demarcate a role for WRN and WRNIP1 in TLS in path-

ways that operate independently of Polθ, and TLS analyses opposite UV lesions have differentiated WRN’s role in TLS in pathways that act independently of Polζ. Altogether, TLS analyses opposite these DNA lesions add clear evidence for the indispensability of WRN and WRNIP1 in

TLS by Y family Pols in conjunction with Rev1 (Supplemental Fig. S1).

TLS by Y family Pols remains functional in the absence of WRN 3' → 5' exonuclease activity

To determine whether WRN's 3' → 5' exonuclease activity was required for TLS, we expressed exonuclease-defective E84A WRN (Huang et al. 1998) in WRN^{-/-} HFs (Supplemental Fig. S2B) and analyzed its effects on TLS opposite *cis-syn* TT dimer, (6-4) TT photoproduct, Tg, or εdA lesions. For each of these DNA lesions, the TLS frequency in WRN^{-/-} HFs expressing E84A WRN remains the same as that in WRN^{-/-} HFs expressing WT WRN (Supplemental Tables S4, S5). Thus, WRN's role in TLS remains functional in the absence of its exonuclease activity, which is likely a structural role in the multiprotein ensemble formation. Consistent with these results, we found that E84A WRN accumulation into replication foci in unirradiated or UV-irradiated cells is identical to that of WT WRN (Supplemental Fig. S7). The persistence of normal levels of TLS in cells expressing E84A WRN gave us the opportunity to determine whether the fidelity of TLS by Y family Pols was affected by this mutation.

Defects in the WRN exonuclease impart high error-proneness on error-free TLS by Polη opposite CPDs

TLS through CPDs is mediated by a Polη-dependent error-free pathway or by Polθ-dependent error-prone pathways (Supplemental Fig. S1A); hence, mutational TLS products do not occur in Polθ-depleted cells (Yoon et al. 2019b). In WRN^{-/-} HFs expressing WT WRN, ~2% of TLS products generated from replication through a *cis-syn* TT dimer harbor a mutational change at either the 3'T or 5'T of the TT dimer (Supplemental Fig. S8A). These mutational products result from Polθ's role in error-prone TLS, as they are absent in Polθ-depleted cells (Supplemental Fig. S8A,B). In WRN^{-/-} HFs expressing E84A WRN, however, the frequency of mutational TLS products increases to ~12% (Supplemental Fig. S8A). Since the Polθ error-prone pathway contributes to ~2% of these mutational TLS products, the remaining ~10% of mutational products would be predicted to derive from Polη's role in TLS (Supplemental Fig. S8B). To affirm this deduction, we analyzed the frequency of mutagenic TLS products in Polθ-depleted WRN^{-/-} HFs expressing E84A WRN in which only the Polη-dependent TLS pathway would be active. In these cells, mutational TLS products occur at a frequency of ~9%, thus validating the inference that in the absence of WRN's exonuclease activity, error-free TLS by Polη through a *cis-syn* TT dimer becomes highly error-prone (Supplemental Fig. S8A,B).

Since CPDs are formed at CC, TC, CT, and TT dipyrimidine sites and since error-prone TLS through CPDs induces C > T and CC > TT signature mutations, we next analyzed the effects of the E84A WRN mutation on UV-induced mutations resulting from TLS through CPDs in the *cII* gene in BBMEFs. In BBMEFs expressing (6-4) PP photolyase, spontaneous mutations occur at a frequency of ~18 × 10⁻⁵ in cells depleted for WRN alone or codepleted for WRN and Polθ

and expressing either the WT WRN or the E84A mutant WRN (Fig. 3A). In UV-irradiated BBMEFs exposed to photo-reactivating light to activate (6-4) PP removal by the (6-4) PP photolyase, depleted for genomic WRN, and expressing WT WRN, mutation frequency rose to ~45 × 10⁻⁵ (Fig. 3A). As we have shown previously (Yoon et al. 2019b), the increase of ~27 × 10⁻⁵ in mutation frequency in UV-irradiated cells over that in unirradiated cells results from error-prone TLS opposite CPDs by Polθ (Fig. 3A,B). In UV-irradiated BBMEFs depleted for WRN and expressing E84A WRN, the mutation frequency rose to ~72 × 10⁻⁵ (Fig. 3A), indicating that in the absence of WRN's exonuclease activity, the frequency of UV-induced mutations resulting from TLS through CPDs increased to ~54 × 10⁻⁵ over that in cells expressing WT WRN ~27 × 10⁻⁵ (Fig. 3A) and implicating that the additional increase in mutation frequency of ~27 × 10⁻⁵ derives from error-prone TLS by Polη (Fig. 3B). To confirm this deduction, we examined UV-induced mutation frequency in BBMEFs codepleted for WRN and Polθ and expressing E84A WRN. Our results showing that mutations occur at a frequency of ~43 × 10⁻⁵ (Fig. 3A) indicated that in the absence of WRN's exonuclease activity, TLS through CPDs by Polη generates mutations at a frequency of ~26 × 10⁻⁵ (Fig. 3A,B). Thus, in the absence of WRN exonuclease activity, the normally error-free TLS through CPDs by Polη becomes as error-prone as TLS mediated by the Polθ-dependent error-prone pathways (Fig. 3B).

In BBMEFs expressing the E84A WRN mutant protein, UV-induced C > T mutations in the *cII* gene resulting from TLS through CPDs are clustered at hotspots at 11 dipyrimidine sequences, similar to those observed in BBMEFs expressing WT WRN (Fig. 4A). In E84A WRN cells, these hotspot mutations derive from the combined action of the Polη- and Polθ-dependent TLS pathways opposite CPDs. To define the spectrum of mutations generated by the Polη pathway, we next examined UV-induced mutations in the *cII* gene in BBMEFs expressing E84A WRN and depleted for Polθ. Whereas no mutational hotspots were observed in Polθ-depleted cells expressing WT WRN (Fig. 4B), in Polθ-depleted cells expressing E84A WRN, mutational hotspots emerged at almost all of the 11 dipyrimidine sites (Fig. 4B). In addition, Polη-generated mutational hotspots exhibit a high prevalence of tandem CC > TT mutations (Fig. 4B). Thus, in the absence of WRN's exonuclease activity, Polη generates C > T mutations at the same dipyrimidine sites in the *cII* gene as Polθ does but also generates tandem mutations.

Defects in WRN exonuclease exacerbate the error-proneness of TLS by Polη and Polθ opposite (6-4) PPs

TLS through (6-4) PPs occurs via error-prone Polη/Polθ or Polι/Polθ pathways in which, following nucleotide insertion opposite the (6-4) PP by Polη or Polι, Polθ would extend synthesis or by an alternative Polζ-dependent error-free pathway (Supplemental Fig. S1B). As we have shown previously (Yoon et al. 2010b, 2021a), or as shown here in WRN^{-/-} HFs expressing WT WRN, ~2% of TLS products resulting from replication through a (6-4) TT

A

Photolyase	siRNA	Vector expressing	UV	Photoreactivation	Mutation frequency (x 10 ⁻⁵)	UV induced ^a mutation frequency (x 10 ⁻⁵)
(6-4)PP Photolyase	WRN	Myc-WT-WRN	-	+	17.5 ± 0.8	-
	WRN	Myc-E84A-WRN	-	+	18.4 ± 0.6	-
	WRN + Polθ	Myc-WT-WRN	-	+	18.6 ± 0.6	-
	WRN + Polθ	Myc-E84A-WRN	-	+	17.4 ± 0.8	-
	WRN	Myc-WT-WRN	+	+	44.5 ± 1.6	27.0
	WRN	Myc-E84A-WRN	+	+	72.6 ± 2.2	54.2
	WRN + Polθ	Myc-WT-WRN	+	+	19.8 ± 1.1	1.2
	WRN + Polθ	Myc-E84A-WRN	+	+	43.4 ± 1.8	26.0
CPD Photolyase	WRN	Myc-WT-WRN	-	+	16.7 ± 0.9	-
	WRN	Myc-E84A-WRN	-	+	15.6 ± 0.7	-
	WRN	Myc-WT-WRN	+	+	28.6 ± 1.4	11.9
	WRN	Myc-E84A-WRN	+	+	44.7 ± 1.6	29.1

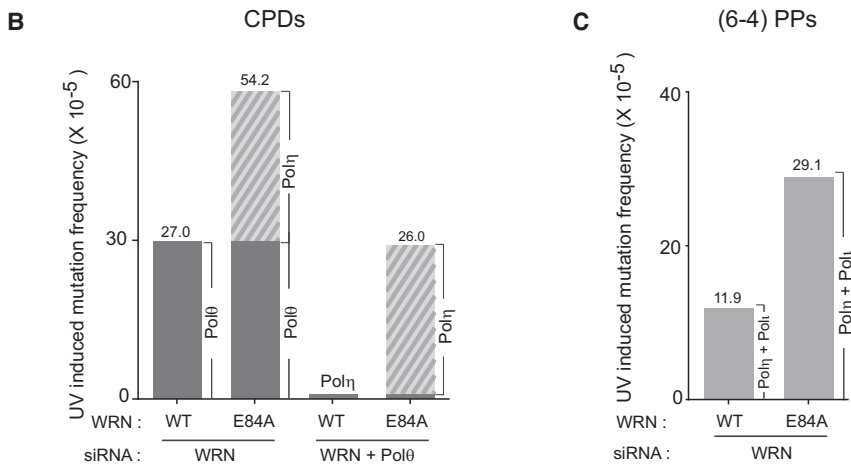


Figure 3. Defects in WRN’s 3’ → 5’ exonuclease activity confer high error-proneness on TLS by Y family Pols opposite UV lesions. (A) UV-induced (5 J/m²) mutation frequencies in the *cII* gene in BBMEFs expressing WT WRN or E84A WRN. UV mutations resulting from TLS opposite CPDs (*top*) were examined in a BBMEF cell line expressing a (6-4) PP photolyase gene, and UV mutations resulting from TLS opposite (6-4) PPs (*bottom*) were examined in a BBMEF cell line expressing a CPD photolyase gene. Mutation frequencies and SEM were calculated from four independent experiments. (a) UV-induced mutation frequencies resulting from TLS through CPDs or (6-4) photoproducts were calculated by subtracting the corresponding spontaneous mutation frequency from the mutation frequency in UV-irradiated cells. (B) Diagrammatic representation of error-proneness imposed by WRN’s exonuclease deficiency upon error-free TLS by Polη opposite CPDs. The figure depicts the error-proneness of Polθ in WRN-depleted BBMEFs expressing WT WRN (mutation frequency 27 × 10⁻⁵) and the elevation in error-proneness (mutation frequency 54.2 × 10⁻⁵) that occurs in BBMEFs expressing E84A WRN due to the added error-proneness of Polη. In BBMEFs codepleted for WRN and Polθ and expressing WT WRN, TLS by Polη operates in an error-free manner, but in BBMEFs expressing E84A WRN, TLS by Polη exhibits high error-proneness (mutation frequency 26 × 10⁻⁵). (C) Diagrammatic representation of elevated error-proneness conferred by WRN’s exonuclease deficiency on TLS by Polη and Polι opposite (6-4) PPs. The figure depicts the increase in error-proneness of TLS by Polη and Polι in WRN-depleted BBMEFs expressing E84A WRN (mutation frequency 29.1 × 10⁻⁵) from that in BBMEFs expressing WT WRN (mutation frequency 11.9 × 10⁻⁵). In B and C, the corresponding spontaneous mutation frequency has been subtracted from the UV-induced mutation frequency; thus, the figures depict mutation frequencies derived from TLS through CPDs (B) or (6-4) PPs (C).

PP harbor a mutational change at the 3’T or 5’T of the photoproduct (Supplemental Fig. S8A). In WRN^{-/-} HFes expressing E84A WRN, the frequency of mutational TLS products rose to ~11%, and the increase in mutation fre-

quency resulted primarily from elevation in the frequency of insertion of G opposite the 3’T (Supplemental Fig. S8A). Thus, in the absence of WRN’s exonuclease activity, Polη- or Polι-dependent TLS opposite (6-4) TT PP manifests an

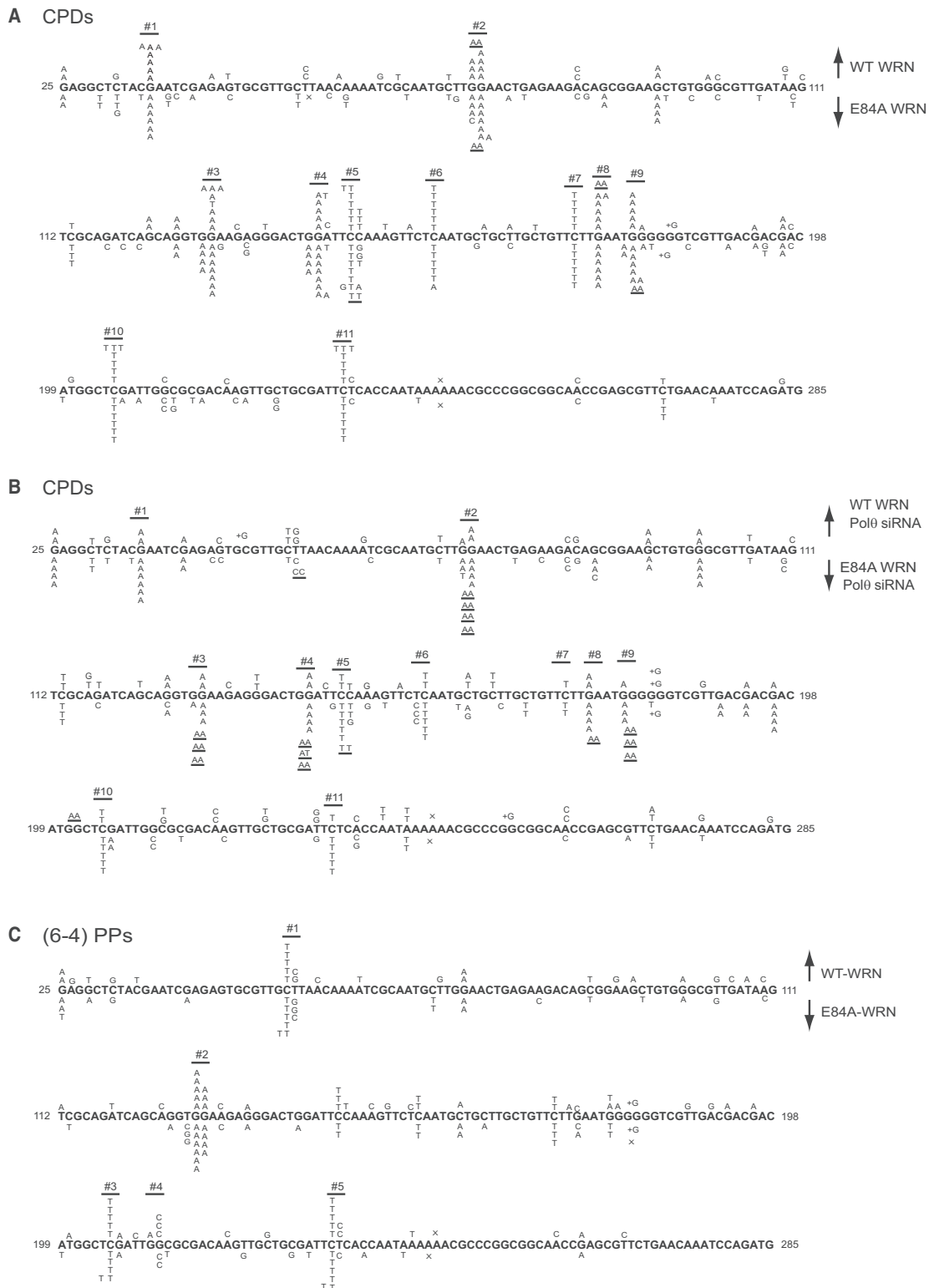


Figure 4. UV-induced (5 J/m^2) mutational spectra in the *cII* gene in BBMEFs resulting from TLS through CPDs or (6-4) PPs. (A) Mutational spectra resulting from TLS through CPDs in WRN-depleted BBMEFs expressing WT WRN are shown *above* the sequence, and those expressing E84A WRN are shown *below* the sequence. (B) Mutational spectra resulting from TLS through CPDs in BBMEFs codepleted for WRN and Pol θ and expressing WT WRN are shown *above* the sequence, and those expressing E84A WRN are shown *below* the sequence. (C) Mutational spectra resulting from TLS through (6-4) PPs in WRN-depleted BBMEFs expressing WT WRN are shown *above* the sequence, and those expressing E84A WRN are shown *below* the sequence. The designations for the other mutational changes are deletion (X), addition (+), and tandem mutations (underlined).

approximately fivefold increase in mutagenicity (Supplemental Fig. S8C).

Next, we examined the effects of the E84A WRN mutation on UV-induced mutations resulting from error-prone TLS by Pol η or Pol ι opposite (6-4) PPs in the *cII* gene in BBMEFs expressing CPD photolyase. In unirradiated cells expressing WT WRN, spontaneous mutations occur at a frequency of $\sim 17 \times 10^{-5}$, and this frequency rises to $\sim 29 \times 10^{-5}$ upon UV irradiation (Fig. 3A). Since CPDs have been removed by the action of CPD photolyase, the increase of $\sim 12 \times 10^{-5}$ in mutation frequency in UV-irradiated cells over that in unirradiated cells (Fig. 3A) resulted from error-prone TLS through (6-4) PPs in WT cells (Fig. 3C). In BBMEFs expressing E84A WRN, UV-induced mutation frequency rose to $\sim 45 \times 10^{-5}$ (Fig. 3A). The additional increase of $\sim 29 \times 10^{-5}$ in mutation frequency in these cells over the spontaneous mutation frequency ($\sim 16 \times 10^{-5}$) gives a measure of error-proneness of TLS mediated by Pol η and Pol ι that occurs in the absence of WRN's exonuclease activity (Fig. 3A,C). Thus, the lack of WRN's exonuclease activity confers an ~ 2.5 -fold increase in the error-proneness of TLS mediated by Pol η or Pol ι opposite (6-4) PPs.

In BBMEFs expressing WT WRN, C > T signature mutations resulting from error-prone TLS by Pol η or Pol ι opposite (6-4) PPs accumulated at hotspots #1, #2, #3, and #5 in the *cII* gene (Fig. 4C; Yoon et al. 2010b, 2021a), and in BBMEFs expressing E84A WRN, the pattern of hotspot mutations in the *cII* gene remained the same as in WT cells (Fig. 4C). This suggests that the WRN nuclease keeps the error rate low by the removal of mismatched nucleotides and that its deficiency does not uncover any pattern of nucleotide misinsertions by Pol η or Pol ι that differs from that in WRN exonuclease-proficient cells.

Defects in WRN exonuclease confer high error-proneness on error-free TLS by Pol κ opposite Tg

TLS opposite the Tg lesion occurs by a Pol κ /Pol ζ -dependent error-free pathway in which, following nucleotide insertion opposite Tg by Pol κ , Pol ζ would extend synthesis. In the alternative pathway, Pol θ conducts error-prone TLS (Supplemental Fig. S1C). Similar to that in WT HF cells (Yoon et al. 2010a, 2014), in WRN $^{-/-}$ HF cells expressing WT WRN, $\sim 2\%$ of TLS products contain a mutational change at the site of Tg, resulting from insertion of G or T opposite it (Fig. 5A,B). In Pol θ -depleted cells expressing WT WRN, mutational TLS products are absent (Fig. 5A,B), and we previously have provided extensive evidence for the lack of mutational TLS products in Pol θ -depleted HF cells (Yoon et al. 2014). Thus, the Pol κ /Pol ζ pathway conducts error-free TLS opposite Tg. We found that in WRN $^{-/-}$ HF cells expressing E84A WRN, the frequency of mutational TLS products rose to $\sim 7\%$ (Fig. 5A,B), suggesting that in the absence of WRN's exonuclease activity, $\sim 5\%$ of mutagenic TLS products were generated by Pol κ , and the remaining $\sim 2\%$ were generated by Pol θ (Fig. 5B). Consistent with this prediction, in Pol θ -depleted WRN $^{-/-}$ HF cells expressing E84A WRN, $\sim 5\%$ of TLS products harbor a mutational change (Fig. 5A,B), confirming manifestation of a high de-

gree of error-proneness by Pol κ , which performs error-free TLS opposite Tg in WT cells.

In Pol θ -depleted WRN $^{-/-}$ HF cells expressing E84A WRN, out of 16 mutational events identified among the 290 TLS products analyzed, four involve a mutational change that would have resulted from the insertion of a G or a T opposite Tg, similar to that in WT cells; the other 12 mutations occur at the nucleotide 5' to the Tg lesion (Fig. 5A and its legend), and these mutations would have resulted from the insertion of a G opposite the T residue present next to Tg on the 5' side, resulting in the 5'TTg > 5'CT mutational change (Fig. 5B). A similar increase in mutations resulting from the insertion of a G opposite the next 5' residue occurs in NC siRNA-treated WRN $^{-/-}$ HF cells expressing E84A WRN (Fig. 5A). The evidence that in the absence of WRN's exonuclease activity, TLS by Pol κ exhibits error-proneness opposite the Tg lesion and, to a larger extent, opposite the next 5' template residue (Fig. 5A,B) implicates a role of Pol κ in inserting nucleotides opposite the Tg lesion as well as opposite the next 5' template residue in human cells (Supplemental Fig. S1C). Thus, Pol ζ would extend synthesis from the nucleotide inserted opposite the next residue on the 5' side of Tg and not from the nucleotide placed opposite Tg.

Defects in WRN exonuclease inflict vast error-proneness on error-free TLS by Pol ι opposite ϵ dA

As shown in Supplemental Figure S1D, TLS opposite ϵ dA operates via an error-free Pol ι /Pol ζ -dependent pathway or by an alternative error-prone Pol θ -dependent pathway. A third pathway dependent on Rev1 polymerase activity, although minor in its overall contribution to TLS, makes a significant contribution to error-prone TLS (Yoon et al. 2019a). In WRN $^{-/-}$ HF cells expressing WT WRN, $\sim 19\%$ of TLS products harbor a mutational change at ϵ dA resulting from misincorporation of predominantly a C and, less frequently, of an A or G opposite ϵ dA (Fig. 5A). In WRN $^{-/-}$ HF cells harboring the vector, the frequency of mutational TLS products declines to $\sim 10\%$ (Fig. 5A). Since both error-free TLS by Pol ι and error-prone TLS by Rev1 polymerase would be inhibited in WRN $^{-/-}$ HF cells (Fig. 5A), these mutational TLS products derive from Pol θ 's role in error-prone TLS. Thus, Pol θ and Rev1 each contribute about equally ($\sim 10\%$) to mutations generated by error-prone TLS opposite ϵ dA in WT cells. In WRN $^{-/-}$ HF cells codepleted for Pol θ and Rev1 and expressing WT WRN and Rev1 protein defective in its polymerase activity (Fig. 5A,C), where only the Pol ι /Pol ζ pathway would be active, no mutational TLS products were observed. This conforms with our previous evidence for Pol ι 's role in error-free TLS opposite ϵ dA (Yoon et al. 2019a). Strikingly, in WRN $^{-/-}$ HF cells expressing E84A WRN, the frequency of mutational TLS products is elevated to $\sim 62\%$ (Fig. 5A,C). Since all the TLS pathways are functional in these cells, and since error-prone TLS by Pol θ would have contributed to $\sim 10\%$ of these mutational TLS products, we presume that the remainder of the mutational TLS products ($\sim 50\%$) resulted from the highly enhanced error-proneness of TLS by Pol ι and/or Rev1. To explore this further, we analyzed the frequency of

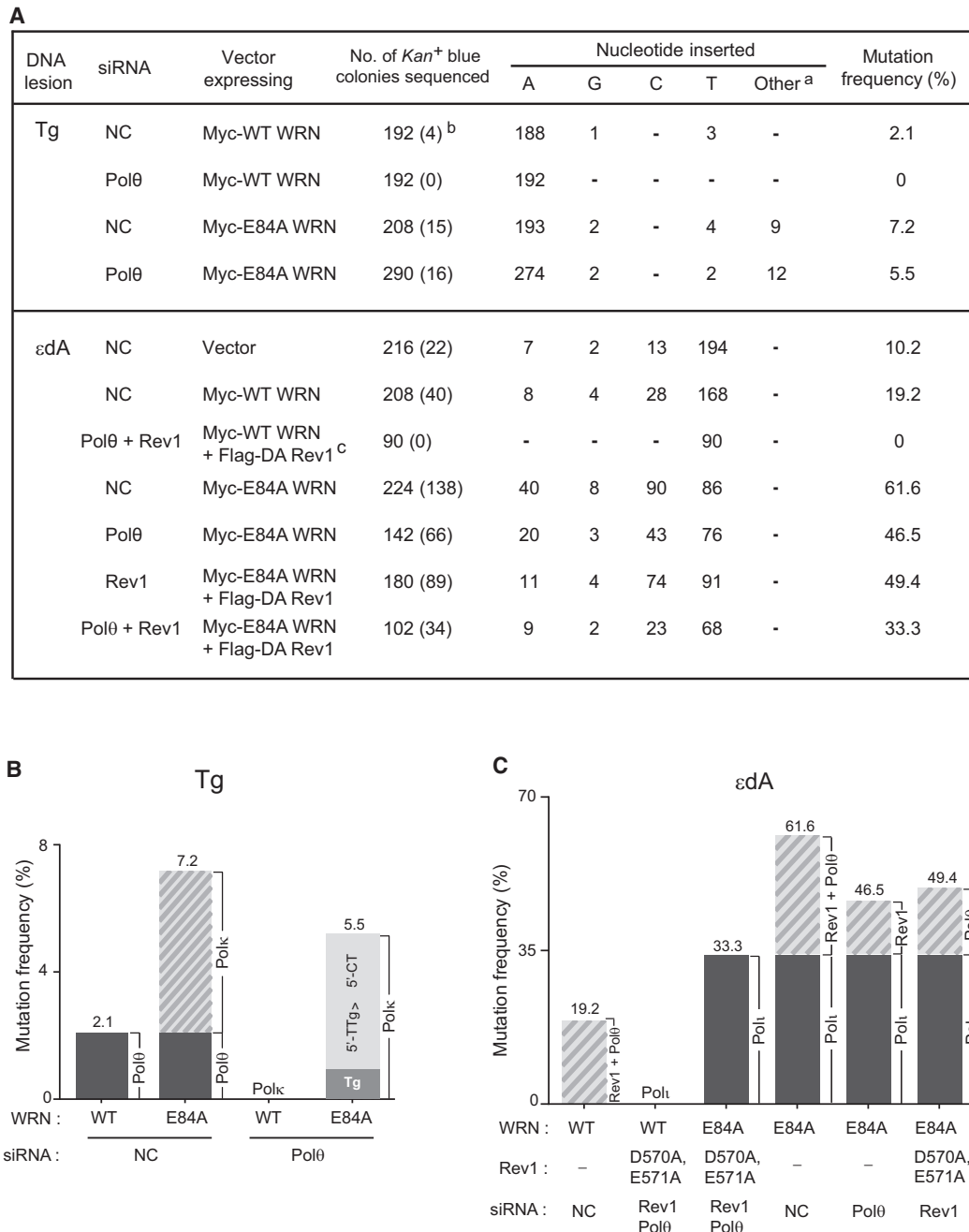


Figure 5. Defects in WRN's 3' → 5' exonuclease activity confer high error-proneness on error-free TLS by Polk opposite Tg and on error-free TLS by Polθ opposite εdA. (A) Effects of E84A WRN on mutation frequencies and nucleotides inserted opposite the Tg (*top*) or the εdA (*bottom*) lesions carried on the leading strand DNA template of a duplex plasmid in WRN^{-/-} HF. (a) In WRN^{-/-} HF treated with control (NC) or Polθ siRNA and expressing E84A WRN, mutations occur at the 5' template residue next to the Tg lesion and involve a change of 5'T > C. Thus, the sequence 5'-CAATTgG-3' is changed to 5'-CAACTG-3' (the corresponding 5' residues are underlined). (b) Numbers in parentheses indicate the total number of mutations. (c) FLAG-DA-Rev1 refers to catalytically inactive D570A E571A Rev1. (B) Diagrammatic representation of error-proneness imposed by WRN's exonuclease deficiency upon error-free TLS by Polk opposite Tg. In WRN^{-/-} HF depleted for Polθ and expressing E84A WRN, error-free TLS by Polk exhibits a mutational pattern in which mutations generated by Polk occur primarily by the change of 5'TTg > 5'CT and less frequently by a change at the Tg lesion site. (C) Diagrammatic representation of highly elevated error-proneness imposed by WRN's exonuclease deficiency upon error-free TLS by Polθ opposite εdA. In WRN^{-/-} HF expressing WT WRN, mutations (~19%) result from error-prone TLS by Rev1 and Polθ. In WRN^{-/-} HF inactivated for both the Rev1 and Polθ error-prone TLS pathways and expressing WT WRN, TLS by Polθ operates in an error-free manner; in striking contrast, expression of E84A WRN in these cells confers a remarkably high error-proneness on Polθ (~33% mutations). Mutation frequency analyses in WRN^{-/-} HF expressing E84A WRN and treated with Polθ siRNA indicate that Rev1's error-proneness is not significantly elevated in the absence of WRN's exonuclease activity.

mutational TLS products in Pol θ -depleted WRN^{-/-} HF cells expressing E84A WRN (Fig. 5A). Our results that mutational TLS products occur at a frequency of ~46% in these cells (Fig. 5A,C) provide a direct measure of the increase in error-proneness that the lack of WRN exonuclease activity confers on TLS by Pol η and/or by Rev1. Next, to demarcate the contribution of Rev1 to the increase in error-prone TLS, we analyzed the incidence of mutational TLS products in Rev1-depleted WRN^{-/-} HF cells expressing E84A WRN and the Rev1 mutant protein defective in its polymerase activity (Fig. 5A). The reduction in the frequency of mutational TLS products to ~49% in these cells from ~62% in WRN^{-/-} HF cells expressing E84A WRN and proficient in Rev1 polymerase activity (Fig. 5A,C) indicates that in cells lacking WRN exonuclease activity, Rev1 polymerase contributes to ~13% of mutagenic TLS products (Fig. 5C), which is about the same as its contribution in WT cells. Since the error-proneness of Rev1 is not perceptibly elevated in the absence of WRN exonuclease function, the large increase in mutation frequency in E84A WRN cells must derive from Pol η 's role in TLS. To verify this inference, we analyzed the frequency of mutational TLS products in WRN^{-/-} HF cells codepleted for Pol θ and Rev1 and expressing E84A WRN and Rev1 catalytic mutant proteins, where only the Pol η -dependent TLS would be functional (Fig. 5A). Our results that mutational TLS products occur at a frequency of ~33% (Fig. 5A,C) show that the absence of WRN exonuclease activity confers remarkably high error-proneness on the normally error-free TLS by Pol η opposite ϵ dA.

Error-prone TLS by Rev1 or Pol θ each generates ~10% mutational products, of which ~6% result from the insertion of a C opposite ϵ dA, and the other ~4% result from the insertion of an A or a G (Fig. 5A). In WRN^{-/-} HF cells codepleted for Rev1 and Pol θ and expressing E84A WRN and Rev1 catalytic mutant proteins (Fig. 5A), Pol η generates ~23% TLS products in which a C is inserted opposite ϵ dA. In addition to a high penchant of Pol η for error-prone TLS opposite ϵ dA by misincorporating a C, Pol η misincorporates an A at a frequency of ~9% or a G at ~2% (Fig. 5A). Thus, the very high intrinsic error-proneness of Pol η opposite this adduct is annulled by the WRN exonuclease activity.

Discussion

WRN and WRNIP1 promote Rev1-dependent replication through DNA lesions in conjunction with Y family Pols

We found that WRN and WRNIP1 along with Rev1 are required for TLS by Y family Pols but are not required for the alternative TLS pathways that do not use Y family Pols. Our results showing that depletion of WRN, WRNIP1, or Rev1 in UV-irradiated WT HF cells confers the same level of reduction in RF progression and that in UV-irradiated WRN^{-/-} HF cells, RF progression is not affected upon depletion of WRNIP1, Rev1, or Pol η but is reduced upon depletion of Pol θ or Pol ζ add evidence for the specificity of WRN and WRNIP1, together with Rev1, in Y family Pol-dependent replication through DNA lesions in the ge-

netic context. Consistent with these results, UV survival is reduced to the same extent upon depletion of WRN, WRNIP1, or Rev1, and UV survival of WRN^{-/-} HF cells is not affected upon depletion of WRNIP1 or Rev1, indicating epistasis.

Previously, the role of WRN and WRNIP1 in TLS has been examined in DT40 chicken cells, which are derived from avian leucosis virus-induced lymphomas. In contrast to the indispensability of WRN, WRNIP1, and Rev1 for TLS by Y family Pols that we observed in human cells (not derived from cancers), WRN's contribution to TLS is minimal in DT40 cells. Thus, whereas Rev1-deficient DT40 cells exhibit a large defect in fork progression through NQO-induced DNA lesions, WRN-deficient cells exhibit reduction in fork progression through NQO lesions similar to that in WT cells. Furthermore, whereas Rev1-deficient DT40 cells suffer a large reduction in UV survival, UV survival of WRN-deficient cells is affected to the same degree as in WT cells (Phillips and Sale 2010). Intriguingly, in DT40 cells, the absence of WRNIP1 suppresses Pol η ^{-/-} TLS defects, and RF progression through UV lesions and UV survival are not affected by the absence of WRNIP1; thus, WRNIP1 plays no direct role in TLS in DT40 cells (Yoshimura et al. 2014). TLS mechanisms in DT40 cells also differ in other ways from those in normal human cells (Yoon et al. 2015); likewise, TLS processes in cells derived from human cancers operate differently than in normal cells (Yoon et al. 2021b)

WRN 3' → 5' exonuclease activity imparts high fidelity on TLS by Y family Pols

The paradox that intrinsically highly error-prone Y family Pol η , Pol ι , or Pol κ conduct predominantly error-free TLS in human cells is resolved by our finding that these Pols function together with WRN, WRNIP1, and Rev1 in TLS. Importantly, WRN's 3' → 5' exonuclease activity makes a pivotal contribution to the high fidelity of TLS by the Y family Pols, as indicated from our evidence that the absence of WRN's 3' → 5' exonuclease activity confers high mutagenicity on the normally error-free TLS by Y family Pols. Thus, Pol η , which performs error-free TLS through CPDs (Yoon et al. 2009, 2019b), manifests high mutagenicity in cells lacking WRN's exonuclease activity such that Pol η -mediated TLS through CPDs formed at the CC, TC, CT, or TT dipyrimidine sites in the *cII* gene in BBMEFs becomes as error-prone as TLS conducted by Pol θ -dependent pathways. Similarly, in the absence of WRN exonuclease activity, the error-proneness of TLS by Pol η and Pol ι opposite (6-4) photoproducts increases, and error-free TLS by Pol κ manifests mutagenicity opposite Tg, adding further evidence for the accentuation of the fidelity of Y family Pols that the removal of misincorporated nucleotides by the WRN exonuclease imparts.

The imposition of extremely high error-proneness on error-free TLS opposite ϵ dA by Pol η in WRN E84A cells reveals an astounding enhancement of fidelity by the WRN exonuclease. Our results showing that the frequency of mutagenic TLS products generated by Pol η in WRN E84A cells

rises to ~33% (in which Pol η inserts a C in ~23% and primarily an A in the remainder of mutagenic TLS products) imply that in TLS together with WRN, WRNIP1, and Rev1, the propensity of Pol η to misinsert a C by Hoogsteen base pairing remains about the same as that indicated from the catalytic efficiency of purified Pol η for inserting a C opposite ϵ dA (Nair et al. 2006a). Thus, the removal of misinserted nucleotides by the WRN exonuclease imparts an enormous increase in the fidelity of TLS opposite ϵ dA by Pol η in human cells such that TLS becomes error-free.

Removal of Y family Pol misinsertions by the WRN 3' \rightarrow 5' exonuclease activity

The critical requirement of WRN's 3' \rightarrow 5' exonuclease activity for the removal of nucleotides misincorporated opposite DNA lesions by the Y family Pols poses the question of how the mismatched primer migrates from the TLS Pol active site to the exonuclease active site in the WRN protein. In the replicative B family DNA polymerases, the 3' \rightarrow 5' exonuclease active site is located ~30–45 Å away from the Pol active site, and a β hairpin in the exonuclease domain keeps the template strand bound to the polymerase domain, while the mismatched primer unwinds from the template and is bound within the exonuclease active site. Thus, the replicative Pols can efficiently switch DNA between the polymerase and exonuclease active sites because of their close proximity within the same protein (Hogg et al. 2007; Darmawan et al. 2015; Jain et al. 2019). The switching of the primer strand from the TLS Pol active site to the exonuclease active site in WRN will require the WRN exonuclease active site to be positioned in close proximity to the TLS Pol active site. Such a proximity could be attained by WRNIP1, Rev1, and/or the other proteins that function together with Y family Pols.

Previously, in a biochemical study with purified WRN and Y family Pols, WRN was shown to stimulate DNA synthesis by Y family Pols on lesion-free and lesion-containing DNA templates by increasing the rate of polymerization; consequently, WRN elevated the extent of nucleotide misincorporation and misextension by Pol η (Kamath-Loeb et al. 2007). In contrast, more efficient removal of the misinserted nucleotide at the G:T mispair compared with that at the G:C base pair by WRN exonuclease prevented mispair formation by Pol η (Maddukuri et al. 2012), and WRN stimulated error-free bypass of 8-oxoG by Pol κ by promoting preferential degradation of the A:8-oxoG mispair (Maddukuri et al. 2014). Additionally, physical interaction of Pol η or Pol κ with purified RecQ C-terminal (RQC) and exo domains of WRN was reported in these studies. However, in pull-down experiments with full-length WRN and Pol η , we found no evidence of direct physical interaction between these proteins. In addition to the above-noted studies with Y family Pols, removal of the 3'-terminal mismatch by WRN exonuclease enabled Pol δ lacking its own proofreading 3' \rightarrow 5' exonuclease activity to extend synthesis from the 3'-terminal mispair (Kamath-Loeb et al. 2012).

WRN exonuclease shares a high degree of structural conservation with the exonuclease domain of *Escherichia coli* DNA Pol I (Perry et al. 2006), and biochemical studies have indicated that WRN exonuclease removes a single 3' mismatched nucleotide more efficiently than a nucleotide from a matched base pair (Kamath-Loeb et al. 1998); hence, the addition of WRN to a DNA polymerase reaction would increase the removal of the misinserted nucleotide. While the proficient removal of the 3'-terminal mismatch by WRN exonuclease would account for the extension of synthesis from the correct base pair by various DNA polymerases in biochemical assays, the specificity of WRN exonuclease action in modulating the fidelity of Y family Pols in cells will be dictated by the proteins that function together with the TLS Pol. Hence, the understanding of the mechanisms that confer high fidelity on Y family Pols will require reconstitution of the TLS process by the Y family Pols—comprised of WRN, WRNIP1, and Rev1 together with Pol η , Pol ι , or Pol κ and possibly other proteins—and analyses of their roles in biochemical and structural studies. It will be of much interest to demarcate the means by which WRN exonuclease gets positioned close to the TLS Pol active site, providing specificity to WRN exonuclease action on the Y family Pol.

Implications of WRN's requirement in TLS by Y family Pols for protection from cancers and aging

WRN has been implicated in a number of cellular processes (Prince et al. 2001; Chu and Hickson 2009; Mukherjee et al. 2018), including a role in lagging strand replication of the G-rich telomeric strand (Crabbe et al. 2004); consequently, acceleration of replicative senescence caused by telomere shortening would contribute to the manifestation of premature aging in WS patients (Chang et al. 2004; Du et al. 2004). Additionally, by promoting Y family Pol-dependent replication through DNA lesions, WRN would protect against replication stress-induced chromosomal instability and the consequent tumorigenesis (Yoon et al. 2019b). Abrogation of Y family Pol-dependent TLS in WRN-deficient cells would contribute to the large variety of cancers—soft tissue sarcoma, osteosarcoma, malignant melanoma, thyroid carcinoma, and skin, lung, and other cancers (Goto et al. 2013)—that arise in WS patients, all of whom lack WRN function. Moreover, by restraining the accumulation of somatic mutations, WRN's role in predominantly error-free TLS by Y family Pols would help retard aging (Goodell and Rando 2015).

Role of TLS in genome stability

Our evidence that the Y family Pols Pol η , Pol ι , or Pol κ function together with Rev1, WRN, and WRNIP1 in TLS; the demonstration that the WRN 3' \rightarrow 5' exonuclease's activity confers an enormous increase in the fidelity of TLS by the Y family Pols opposite different types of DNA lesions; and the possibility that the fidelity of Y family Pols is elevated further via mechanisms that curtail nucleotide misincorporation by these Pols identify a means

through which low-fidelity TLS Pols have been adapted to perform TLS with a vastly enhanced fidelity. The evolutionary adaptation of TLS Pols to act in a predominantly error-free manner would provide a safeguard against genome instability rather than contribute to it, as is commonly perceived in light of the intrinsically high error-proneness of monomeric purified TLS Pols. In addition, the evidence that both error-free TLS by Pol η and error-prone TLS by Pol θ through UV lesions protect against replication stress-induced chromosomal instability and skin cancer formation implicates a role of TLS mechanisms in providing a greater measure of protection against genome instability than processes such as sister chromatid exchange and nonhomologous end joining, which operate in the absence of TLS (Yoon et al. 2019b). Thus, by largely attenuating the error-proneness of TLS Pols and by avoiding the formation of chromosomal aberrations, TLS mechanisms would account for a large measure of genome stability and protection from tumorigenesis.

Materials and methods

Cell lines and cell culture

SV40 transformed WT human fibroblast (GM00637) and XPA human fibroblast (GM04429) cell lines were obtained from Coriell Institute Cell Repository. A WRN-deficient AG11395 cell line (Dhillon et al. 2007) derived from AG00780G fibroblasts taken from a 60-yr-old male WS patient (Saito and Moses 1991) was obtained from Coriell Institute Cell Repository. AG00780G cells are homozygous for a 1336 C > T mutation that leads to premature translation termination (Dhillon et al. 2007). We refer to these WRN-deficient cells as WRN^{-/-}. Big blue mouse embryonic fibroblasts (BBMEFs) were obtained from Agilent. Cells were grown on plastic culture dishes at 37°C in a humidified incubator with 5% CO₂ in DMEM (GenDepot) containing 10% fetal bovine serum (GenDepot) and 1% antibiotic-antimycotic (GenDepot).

Construction of plasmid vectors containing a cis-syn TT dimer, a (6-4) TT photoproduct, thymine glycol (Tg), or a 1,N⁶-ethenodeoxyadenosine (edA)

The heteroduplex vectors containing a *cis-syn* TT dimer, a (6-4) TT photoproduct, a Tg, or an edA on the leading or lagging strand template were constructed as described previously (Yoon et al. 2009, 2010a,b, 2019a).

Translesion synthesis assays in human cells

For siRNA knockdown of WRN or WRNIP1, HPLC-purified duplex siRNA for human genes were purchased from Thermo Fisher Scientific. The sense sequence of the WRN siRNA target sequence was 5'-GCAAAUGUUACUUG UUCA-3', and the sense sequence of the WRNIP1 siRNA target sequence was 5'-GAAACAUAGCAUAAG GUUU-3'. The efficiency of siRNA knockdown was verified by Western blot analysis (Supplemental Fig. S2). The

siRNA knockdown efficiency of other TLS Pols as well as the detailed methods for TLS assay have been described previously (Yoon et al. 2009, 2015).

Focus formation assay

For analyses of UV-induced foci for Pol η , Pol ι , Pol κ , Rev7, WRN, or WRNIP1, GM00637 HF cells were treated with siRNA and cultured on a coverslip with 50% confluence. For Rev1 focus analysis, GM00637 HF cells stably expressing FLAG-Rev1 were treated with siRNA and cultured on a coverslip with 50% confluence. After 48 h, cells were treated with 30 J/m² UVC. For wild-type-WRN or E84A WRN focus analysis, AG11395 cells stably expressing myc-wild-type-WRN or myc-E84A-WRN were cultured on a coverslip with 70% confluence. Cells were treated with 30 J/m² UVC. After UV irradiation, fresh growth media were added and incubated for 4 h. After washing with PBS buffer, cells were pre-extracted in 0.2% Triton X-100 for 2 min and fixed with 4% paraformaldehyde for 20 min. Cells were incubated in blocking buffer and 2% BSA in PBS containing 0.2% Tween20 (PBST) for 1 h. Primary antibodies (mouse anti-FLAG antibody [Sigma], rabbit anti-Pol η antibody [Bethyl Laboratories], rabbit anti-Pol ι antibody [Bethyl Laboratories], rabbit anti-Pol κ antibody [Bethyl Laboratories], mouse anti-Rev7 antibody [BD Biosciences], rabbit anti-WRNIP1 antibody [Novus Biologicals], and mouse anti-WRN antibody [Cell Signaling]) were diluted in blocking buffer and incubated for 1 h, followed by a wash with PBST buffer. Secondary antibodies (goat antimouse Alexa 488 [Invitrogen] or goat antirabbit Alexa 488 [Invitrogen]) were applied for 30 min, and coverslips were mounted with antifade Gold mounting media (Invitrogen). Nuclear staining was performed with DAPI (Molecular Probes) in PBS buffer for 20 min. The fluorescent images were visualized and captured by fluorescence microscopy (Nikon Eclipse 80i).

For analysis of cisplatin-induced foci, GM00637 HF cells were treated with siRNA and cultured on a coverslip with 50% confluence. After 48 h, cells were treated with 60 μ M cisplatin (Sigma) for 4 h. For Rev1 focus analysis, we used rabbit anti-Rev1 antibody (Sigma).

Coimmunoprecipitation of proteins in chromatin extracts

GM00637 HF cells stably expressing FLAG-Rev1 were cultured in 15-cm plates with ~80% confluence. Cells were washed with PBS buffer and irradiated with 30 J/m² UVC in the presence of PBS buffer. After UV irradiation, cells were incubated in growth media for 4 h. For chromatin-bound nuclear extracts, cells were lysed with CSK (cytoskeleton) buffer (10 mM HEPES at pH 6.8, 100 mM NaCl, 300 mM sucrose, 3 mM MgCl₂, 0.5% Triton X-100, e-complete protease inhibitors), and chromatin extracts were treated with 1% formalin in PBS buffer for 10 min at room temperature followed by the addition of 125 mM glycine. Cell pellets were resuspended in PBS buffer containing 30 U of Xpernase (GenDepot). Extracts were incubated for 10 min at room temperature and

then centrifuged to isolate the chromatin extracts. Two milligrams of chromatin extracts was diluted with an equal volume of immunoprecipitation (IP) buffer (150 mM NaCl, 50 mM Tris-HCl at pH 7.5, 1 mM EDTA, 0.05% NP40, 10% glycerol, protease inhibitors) and mixed with 0.5 μ g of FLAG agarose beads overnight at 4° C. FLAG agarose beads were washed twice with IP buffer, and bound proteins were eluted in Laemmli buffer (2% SDS, 10% glycerol, 60 mM Tris-HCl at pH 6.8, 100 mM DTT, 0.05% bromophenol blue). WRN antibody (Novus Biologicals), WRNIP1 antibody (Novus Biologicals), Pol η antibody (Bethyl Laboratories), or FLAG antibody (Sigma) was used for Western blot analysis.

Western blot analysis

Forty-eight hours after siRNA transfection, cells were washed with PBS buffer and lysed with RIPA buffer (1 \times PBS, 1% IP-40, 0.5% sodium deoxycholate, 0.1% SDS). After 1 h of incubation on ice, the cellular mixture was centrifuged and the supernatant was collected. Equivalent amounts (~30 μ g) of prepared cellular extracts were separated on a 10% SDS–polyacrylamide gel and transferred to a PVDF membrane (Bio-Rad). The membranes were probed with rabbit anti-WRN (Novus Biologicals), anti-WRNIP1 (Novus Biologicals), anti-Rev1 (Sigma), or anti-Myc (Santa Cruz Biotechnology) antibodies, followed by appropriate secondary antibodies conjugated with horseradish peroxidase. The signals were detected using ECL-Plus (GenDepot). For the loading control, anti- α -tubulin antibody (Santa Cruz Biotechnology), anti-LaminB1 antibody (Abcam), or anti- β tubulin antibody (Cell Signaling Technology) was used.

Big blue transgenic mouse cell line and siRNA knockdown

The big blue transgenic mouse embryonic fibroblast (BBMEF) cells were grown in DMEM containing 10% FBS (GenDepot) and antibiotics. HPLC-purified duplex siRNA for mouse WRN was purchased from Thermo Fisher Scientific. The sense sequence of mWRN siRNA was 5'-GCAAUUAUUUGCCUCAAG-3', and the efficiency of its knockdown was verified by Western blot analysis. For the *cII* mutation assay, cells were plated on 100-mm plates at 50% confluence (~5 \times 10⁶ cells), and 500 pmol of synthetic duplex siRNAs was transfected using 50 μ L of iMfectin transfection reagent (GenDepot) following the manufacturer's instructions.

UV irradiation, photoreactivation, and *cII* mutational assays in siRNA-treated BBMEF cells

Forty-eight hours after siRNA knockdown, cells were washed with HBSS buffer (Invitrogen) and irradiated at 5 J/m² with UVC light, followed by photoreactivation for 3 h at room temperature as previously described (Yoon et al. 2009, 2010b). Fresh growth medium was then added and cells were incubated for 24 h, after which the second siRNA transfection was carried out to maintain the siRNA

knockdown of the target gene(s). Cells were incubated for an additional 4 d to allow for mutation fixation. Mouse genomic DNA was isolated using the genomic DNA isolation kit (Qiagen). The LIZ shuttle vector was rescued from the genomic DNA by mixing DNA aliquots and Transpack packaging extract (Stratagene), and the *cII* assay was carried out as previously described (Yoon et al. 2009, 2010b). Mutation frequency was calculated by dividing the number of mutant plaques by the number of total plaques. For mutation analysis, the sequences of PCR products of the *cII* gene from the mutant plaques were analyzed as described previously (Yoon et al. 2009, 2010b).

DNA fiber assay

GM00637 HF or WRN^{-/-} HF cells were transfected with 100 pmol of siRNAs, and 48 h after siRNA transfection, cells were pulse-labeled with 25 μ M IdU (Sigma) for 20 min. Cells were then washed twice with PBS buffer and irradiated with 10 J/m² UVC. After UV irradiation, cells were labeled with 250 μ M CldU for 20 min. DNA fibers were spread on glass slides, and slides were incubated in 2.5 M HCl for 90 min and then washed with PBS buffer. The slides were incubated in blocking buffer and 5% BSA in PBS for 2 h. Primary antibodies (rat anti-BrdU antibody [Abcam] and mouse anti-BrdU antibody [BD Biosciences]) were diluted in blocking buffer and incubated for 1 h, followed by extensive washing with PBS buffer. Secondary antibodies (goat anti-rat Alexa 594 and goat anti-mouse Alexa 488) were applied for 30 min, and slides were mounted with antifade Gold mounting media (Invitrogen). Fibers were analyzed using a Nikon Eclipse fluorescence microscope.

UV survival assay

GM00637 HF or WRN^{-/-} HF cells were transfected with siRNAs, and 48 h after siRNA transfection, cells were treated with UV. For UV irradiation, cells were washed with PBS buffer and irradiated with various doses (0–20 J/m²) of UVC light in the presence of PBS buffer. After irradiation, fresh growth media were added and cells were incubated for an additional 48 h. UV cytotoxicity was determined by MTS assay (Promega). Briefly, 100 μ L of MTS assay solution was added to each well and incubated for 30 min. Cell viability was determined by measuring OD at 490 nm; four independent experiments were performed.

Stable expression of myc-wild-type-WRN or myc-E84A-WRN in WRN^{-/-} HF or BBMEFs

Plasmids containing myc-wild-type-WRN or myc-E84A-WRN were obtained from the Raymond Monnat Laboratory (University of Washington, Seattle). The vectors were transfected into WRN^{-/-} AG11395 HF or BBMEFs by iMfectin transfection reagent (GenDepot). After 24 h of incubation, 2 μ g of puromycin (Thermo Fisher Scientific) was added to the culture media. After 3 d of incubation, cells were washed with PBS buffer and continuously cultured with the media containing 1 μ g of puromycin for

~2 wk. Protein expression and siRNA knockdown efficiency were verified by Western blot analysis (Supplemental Fig. S2).

Stable expression of FLAG-D570A E571A Rev1 in WRN^{-/-} HF cells stably expressing myc-wild type-WRN or myc-E84A-WRN

Plasmids containing FLAG-D570A E571A Rev1 were transfected into WRN^{-/-} HF cells stably expressing myc-wild-type-WRN or myc-E84A-WRN by iMfectin transfection reagent (GenDepot). After 24 h of incubation, 50 µg of zeocin (Thermo Fisher Scientific) was added to the culture media. After 3 d of incubation, cells were washed with PBS buffer and continuously cultured for ~2 wk with media containing 25 µg of zeocin and 1 µg of puromycin on plastic culture dishes at 37°C in a humidified incubator with 5% CO₂. Protein expression was verified by Western blot analysis.

Data availability

All of the study data are included in the tables and figures here and in the Supplemental Material.

Competing interest statement

The authors declare no competing interests.

Acknowledgments

We thank Robert Johnson and Mariano Garcia-Blanco for reading the manuscript and for helpful suggestions. We are grateful to Raymond Monnat for the plasmid-carrying myc-WT WRN and myc-E84A WRN. This work was supported by National Institutes of Health grants R01 GM126087 and R35 GM148364 to L.P.

Author contributions: J.-H.Y. performed the experiments and analyzed the data. K.S. performed immunoprecipitation experiments and contributed to other experiments. L.P. and S.P. designed and coordinated the study. J.-H.Y., L.P., and S.P. wrote the manuscript.

References

Alexandrov LB, Nik-Zainal S, Wedge DC, Aparicio SA, Behjati S, Biankin AV, Bignell GR, Bolli N, Borg A, Børresen-Dale AL, et al. 2013. Signatures of mutational processes in human cancer. *Nature* **500**: 415–421. doi:10.1038/nature12477

Besaratinia A, Pfeifer GP. 2006. Investigating human cancer etiology by DNA lesion footprinting and mutagenicity analysis. *Carcinogenesis* **27**: 1526–1537. doi:10.1093/carcin/bgi311

Biertümpfel C, Zhao Y, Kondo Y, Ramon-Maiques S, Gregory M, Lee JY, Masutani C, Lehmann AR, Hanaoka F, Yang W. 2010. Structure and mechanism of human DNA polymerase η . *Nature* **465**: 1044–1048. doi:10.1038/nature09196

Chang S, Multani AS, Cabrera NG, Naylor ML, Laud P, Lombard D, Pathak S, Guarente L, DePinho RA. 2004. Essential role of

limiting telomeres in the pathogenesis of Werner syndrome. *Nat Genet* **36**: 877–882. doi:10.1038/ng1389

Choudhary S, Sommers JA, Brosh RM Jr. 2004. Biochemical and kinetic characterization of the DNA helicase and exonuclease activities of Werner syndrome protein. *J Biol Chem* **279**: 34603–34613. doi:10.1074/jbc.M401901200

Chu WK, Hickson ID. 2009. RecQ helicases: multifunctional genome caretakers. *Nat Rev Cancer* **9**: 644–654. doi:10.1038/nrc2682

Conde J, Yoon JH, Roy Choudhury J, Prakash L, Prakash S. 2015. Genetic control of replication through N1-methyladenine in human cells. *J Biol Chem* **290**: 29794–29800. doi:10.1074/jbc.M115.693010

Crabbe L, Verdun RE, Haggblom CI, Karlseder J. 2004. Defective telomere lagging strand synthesis in cells lacking WRN helicase activity. *Science* **306**: 1951–1953. doi:10.1126/science.1103619

Darmawan H, Harrison M, Reha-Krantz LJ. 2015. DNA polymerase 3'→5' exonuclease activity: different roles of the β hairpin structure in family-B DNA polymerases. *DNA Repair (Amst)* **29**: 36–46. doi:10.1016/j.dnarep.2015.02.014

Dhillon KK, Sidorova J, Saintigny Y, Poot M, Gollahon K, Rabinovitch PS, Monnat RJ Jr. 2007. Functional role of the Werner syndrome RecQ helicase in human fibroblasts. *Aging Cell* **6**: 53–61. doi:10.1111/j.1474-9726.2006.00260.x

Du X, Shen J, Kugan N, Furth EE, Lombard DB, Cheung C, Pak S, Luo G, Pignolo RJ, DePinho RA, et al. 2004. Telomere shortening exposes functions for the mouse Werner and Bloom syndrome genes. *Mol Cell Biol* **24**: 8437–8446. doi:10.1128/MCB.24.19.8437-8446.2004

Fu W, Ligabue A, Rogers KJ, Akey JM, Monnat RJ Jr. 2017. Human RECQ helicase pathogenic variants, population variation and “missing” diseases. *Hum Mutat* **38**: 193–203. doi:10.1002/humu.23148

Goodell MA, Rando TA. 2015. Stem cells and healthy aging. *Science* **350**: 1199–1204. doi:10.1126/science.aab3388

Goto M, Ishikawa Y, Sugimoto M, Furuichi Y. 2013. Werner syndrome: a changing pattern of clinical manifestations in Japan (1917–2008). *Biosci Trends* **7**: 13–22.

Gray MD, Shen J-C, Kamath-Loeb AS, Blank A, Sopher BL, Martin GM, Oshima J, Loeb LA. 1997. The Werner syndrome protein is a DNA helicase. *Nat Genet* **17**: 100–103. doi:10.1038/ng0997-100

Hogg M, Aller P, Konigsberg W, Wallace SS, Doublé S. 2007. Structural and biochemical investigation of the role in proof-reading of a β hairpin loop found in the exonuclease domain of a replicative DNA polymerase of the B family. *J Biol Chem* **282**: 1432–1444. doi:10.1074/jbc.M605675200

Huang S, Li B, Gray MD, Oshima J, Mian IS, Campisi J. 1998. The premature ageing syndrome protein, WRN, is a 3'→5' exonuclease. *Nat Genet* **20**: 114–116. doi:10.1038/2410

Huang S, Beresten S, Li B, Oshima J, Ellis NA, Campisi J. 2000. Characterization of the human and mouse WRN 3'→5' exonuclease. *Nucleic Acids Res* **28**: 2396–2405. doi:10.1093/nar/28.12.2396

Huang S, Lee L, Hanson NB, Lenaerts C, Hoehn H, Poot M, Rubin CD, Chen DF, Yang CC, Juch H, et al. 2006. The spectrum of WRN mutations in Werner syndrome patients. *Hum Mutat* **27**: 558–567. doi:10.1002/humu.20337

Jain R, Rice WJ, Malik R, Johnson RE, Prakash L, Prakash S, Ubarretxena-Belandia I, Aggarwal AK. 2019. Cryo-EM structure and dynamics of eukaryotic DNA polymerase δ holoenzyme. *Nat Struct Mol Biol* **26**: 955–962. doi:10.1038/s41594-019-0305-z

- Johnson RE, Prakash S, Prakash L. 1999. Efficient bypass of a thymine-thymine dimer by yeast DNA polymerase, Pol η . *Science* **283**: 1001–1004. doi:10.1126/science.283.5404.1001
- Johnson RE, Washington MT, Haracska L, Prakash S, Prakash L. 2000a. Eukaryotic polymerases ι and ζ act sequentially to bypass DNA lesions. *Nature* **406**: 1015–1019. doi:10.1038/35023030
- Johnson RE, Washington MT, Prakash S, Prakash L. 2000b. Fidelity of human DNA polymerase η . *J Biol Chem* **275**: 7447–7450. doi:10.1074/jbc.275.11.7447
- Johnson RE, Haracska L, Prakash S, Prakash L. 2001. Role of DNA polymerase η in the bypass of a (6-4) TT photoproduct. *Mol Cell Biol* **21**: 3558–3563. doi:10.1128/MCB.21.10.3558-3563.2001
- Johnson RE, Prakash L, Prakash S. 2005. Distinct mechanisms of *cis*-*syn* thymine dimer bypass by Dpo4 and DNA polymerase η . *Proc Natl Acad Sci* **102**: 12359–12364. doi:10.1073/pnas.0504380102
- Kamath-Loeb AS, Shen JC, Loeb LA, Fry M. 1998. Werner syndrome protein. II. characterization of the integral 3'→5' DNA exonuclease. *J Biol Chem* **273**: 34145–34150. doi:10.1074/jbc.273.51.34145
- Kamath-Loeb AS, Lan L, Nakajima S, Yasui A, Loeb LA. 2007. Werner syndrome protein interacts functionally with translesion DNA polymerases. *Proc Natl Acad Sci* **104**: 10394–10399. doi:10.1073/pnas.0702513104
- Kamath-Loeb AS, Shen JC, Schmitt MW, Loeb LA. 2012. The Werner syndrome exonuclease facilitates DNA degradation and high fidelity DNA polymerization by human DNA polymerase δ . *J Biol Chem* **287**: 12480–12490. doi:10.1074/jbc.M111.332577
- Kawabe Y, Branzei D, Hayashi T, Suzuki H, Masuko T, Onoda F, Heo SJ, Ikeda H, Shimamoto A, Furuichi Y, et al. 2001. A novel protein interacts with the Werner's syndrome gene product physically and functionally. *J Biol Chem* **276**: 20364–20369. doi:10.1074/jbc.C100035200
- Lauper JM, Krause A, Vaughan TL, Monnat RJ Jr. 2013. Spectrum and risk of neoplasia in Werner syndrome: a systematic review. *PLoS One* **8**: e59709. doi:10.1371/journal.pone.0059709
- Lebel M, Monnat RJ Jr. 2018. Werner syndrome (WRN) gene variants and their association with altered function and age-associated diseases. *Ageing Res Rev* **41**: 82–97. doi:10.1016/j.arr.2017.11.003
- Maddukuri L, Ketkar A, Eddy S, Zafar MK, Griffin WC, Eoff RL. 2012. Enhancement of human DNA polymerase η activity and fidelity is dependent upon a bipartite interaction with the Werner syndrome protein. *J Biol Chem* **287**: 42312–42323. doi:10.1074/jbc.M112.410332
- Maddukuri L, Ketkar A, Eddy S, Zafar MK, Eoff RL. 2014. The Werner syndrome protein limits the error-prone 8-oxo-dG lesion bypass activity of human DNA polymerase κ . *Nucleic Acids Res* **42**: 12027–12040. doi:10.1093/nar/gku913
- Martincorena I, Roshan A, Gerstung M, Ellis P, Van Loo P, McLaren S, Wedge DC, Fullam A, Alexandrov LB, Tubio JM, et al. 2015. Tumor evolution. High burden and pervasive positive selection of somatic mutations in normal human skin. *Science* **348**: 880–886. doi:10.1126/science.aaa6806
- Masutani C, Kusumoto R, Yamada A, Dohmae N, Yokoi M, Yuasa M, Araki M, Iwai S, Takio K, Hanaoka F. 1999. The XPV (xeroderma pigmentosum variant) gene encodes human DNA polymerase η . *Nature* **399**: 700–704. doi:10.1038/21447
- Mukherjee S, Sinha D, Bhattacharya S, Srinivasan K, Abdilsalaam S, Asaithamby A. 2018. Werner syndrome protein and DNA replication. *Int J Mol Sci* **19**: 3442. doi:10.3390/ijms19113442
- Nair DT, Johnson RE, Prakash S, Prakash L, Aggarwal AK. 2004. Replication by human DNA polymerase- ι occurs by Hoogsteen base-pairing. *Nature* **430**: 377–380. doi:10.1038/nature02692
- Nair DT, Johnson RE, Prakash L, Prakash S, Aggarwal AK. 2005. Human DNA polymerase ι incorporates dCTP opposite template G via a G.C⁺ Hoogsteen base pair. *Structure* **13**: 1569–1577. doi:10.1016/j.str.2005.08.010
- Nair DT, Johnson RE, Prakash L, Prakash S, Aggarwal AK. 2006a. Hoogsteen base pair formation promotes synthesis opposite the 1,N6-ethenodeoxyadenosine lesion by human DNA polymerase ι . *Nat Struct Mol Biol* **13**: 619–625. doi:10.1038/nsmb1118
- Nair DT, Johnson RE, Prakash S, Prakash L, Aggarwal AK. 2006b. An incoming nucleotide imposes an *anti* to *syn* conformational change on the templating purine in the human DNA polymerase- ι active site. *Structure* **14**: 749–755. doi:10.1016/j.str.2006.01.010
- Newman JA, Gavard AE, Lieb S, Ravichandran MC, Hauer K, Werni P, Geist L, Böttcher J, Engen JR, Rumpel K, et al. 2021. Structure of the helicase core of Werner helicase, a key target in microsatellite instability cancers. *Life Sci Alliance* **4**: e202000795. doi:10.26508/lsa.202000795
- Oshima J, Sidorova JM, Monnat RJ Jr. 2017. Werner syndrome: clinical features, pathogenesis and potential therapeutic interventions. *Ageing Res Rev* **33**: 105–114. doi:10.1016/j.arr.2016.03.002
- Perry JJ, Yannone SM, Holden LG, Hitomi C, Asaithamby A, Han S, Cooper PK, Chen DJ, Tainer JA. 2006. WRN exonuclease structure and molecular mechanism imply an editing role in DNA end processing. *Nat Struct Mol Biol* **13**: 414–422. doi:10.1038/nsmb1088
- Pfeifer GP. 1997. Formation and processing of UV photoproducts: effects of DNA sequence and chromatin environment. *Photochem Photobiol* **65**: 270–283. doi:10.1111/j.1751-1097.1997.tb08560.x
- Phillips LG, Sale JE. 2010. The Werner's syndrome protein collaborates with REV1 to promote replication fork progression on damaged DNA. *DNA Repair (Amst)* **9**: 1064–1072. doi:10.1016/j.dnarep.2010.07.006
- Prakash S, Prakash L. 2002. Translesion DNA synthesis in eukaryotes: a one- or two-polymerase affair. *Genes Dev* **16**: 1872–1883. doi:10.1101/gad.1009802
- Prakash S, Johnson RE, Prakash L. 2005. Eukaryotic translesion synthesis DNA polymerases: specificity of structure and function. *Ann Rev Biochem* **74**: 317–353. doi:10.1146/annurev.biochem.74.082803.133250
- Prince PR, Emond MJ, Monnat RJ Jr. 2001. Loss of Werner syndrome protein function promotes aberrant mitotic recombination. *Genes Dev* **15**: 933–938. doi:10.1101/gad.877001
- Saito H, Moses RE. 1991. Immortalization of Werner syndrome and progeria fibroblasts. *Exp Cell Res* **192**: 373–379. doi:10.1016/0014-4827(91)90054-X
- Shen JC, Gray MD, Oshima J, Loeb LA. 1998. Characterization of Werner syndrome protein DNA helicase activity: directionality, substrate dependence and stimulation by replication protein A. *Nucleic Acids Res* **26**: 2879–2885. doi:10.1093/nar/26.12.2879
- Silverstein TD, Johnson RE, Jain R, Prakash L, Prakash S, Aggarwal AK. 2010. Structural basis for the suppression of skin cancers by DNA polymerase η . *Nature* **465**: 1039–1043. doi:10.1038/nature09104
- Tsurimoto T, Shinozaki A, Yano M, Seki M, Enomoto T. 2005. Human Werner helicase interacting protein 1 (WRNIP1)

- functions as a novel modulator for DNA polymerase δ . *Genes Cells* **10**: 13–22. doi:10.1111/j.1365-2443.2004.00812.x
- Washington MT, Johnson RE, Prakash L, Prakash S. 2002. Human *DINB1*-encoded DNA polymerase κ is a promiscuous extender of mispaired primer termini. *Proc Natl Acad Sci* **99**: 1910–1914. doi:10.1073/pnas.032594399
- Yokote K, Chanprasert S, Lee L, Eirich K, Takemoto M, Watanabe A, Koizumi N, Lessel D, Mori T, Hisama FM, et al. 2017. *WRN* mutation update: mutation spectrum, patient registries, and translational prospects. *Hum Mutat* **38**: 7–15. doi:10.1002/humu.23128
- Yoon J-H, Lee CS, O'Connor TR, Yasui A, Pfeifer GP. 2000. The DNA damage spectrum produced by simulated sunlight. *J Mol Biol* **299**: 681–693. doi:10.1006/jmbi.2000.3771
- Yoon J-H, Prakash L, Prakash S. 2009. Highly error-free role of DNA polymerase η in the replicative bypass of UV-induced pyrimidine dimers in mouse and human cells. *Proc Natl Acad Sci* **106**: 18219–18224. doi:10.1073/pnas.0910121106
- Yoon J-H, Bhatia G, Prakash S, Prakash L. 2010a. Error-free replicative bypass of thymine glycol by the combined action of DNA polymerases κ and ζ in human cells. *Proc Natl Acad Sci* **107**: 14116–14121. doi:10.1073/pnas.1007795107
- Yoon J-H, Prakash L, Prakash S. 2010b. Error-free replicative bypass of (6-4) photoproducts by DNA polymerase ζ in mouse and human cells. *Genes Dev* **24**: 123–128. doi:10.1101/gad.1872810
- Yoon JH, Prakash S, Prakash L. 2012. Genetic control of translesion synthesis on leading and lagging DNA strands in plasmids derived from Epstein-Barr virus in human cells. *MBio* **3**: e00271-12. doi:10.1128/mBio.00271-12
- Yoon JH, Roy Choudhury J, Park J, Prakash S, Prakash L. 2014. A role for DNA polymerase θ in promoting replication through oxidative DNA lesion, thymine glycol, in human cells. *J Biol Chem* **289**: 13177–13185. doi:10.1074/jbc.M114.556977
- Yoon JH, Park J, Conde J, Wakamiya M, Prakash L, Prakash S. 2015. Rev1 promotes replication through UV lesions in conjunction with DNA polymerases η , ι , and κ but not DNA polymerase ζ . *Genes Dev* **29**: 2588–2602. doi:10.1101/gad.272229.115
- Yoon JH, Roy Choudhury J, Park J, Prakash S, Prakash L. 2017. Translesion synthesis DNA polymerases promote error-free replication through the minor-groove DNA adduct 3-deaza-3-methyladenine. *J Biol Chem* **292**: 18682–18688. doi:10.1074/jbc.M117.808659
- Yoon JH, Hodge RP, Hackfeld LC, Park J, Roy Choudhury J, Prakash S, Prakash L. 2018. Genetic control of predominantly error-free replication through an acrolein-derived minor-groove DNA adduct. *J Biol Chem* **293**: 2949–2958. doi:10.1074/jbc.RA117.000962
- Yoon JH, Johnson RE, Prakash L, Prakash S. 2019a. DNA polymerase θ accomplishes translesion synthesis opposite 1,N⁶-ethenodeoxyadenosine with a remarkably high fidelity in human cells. *Genes Dev* **33**: 282–287. doi:10.1101/gad.320531.118
- Yoon JH, McArthur MJ, Park J, Basu D, Wakamiya M, Prakash L, Prakash S. 2019b. Error-prone replication through UV lesions by DNA polymerase θ protects against skin cancers. *Cell* **176**: 1295–1309.e15. doi:10.1016/j.cell.2019.01.023
- Yoon JH, Basu D, Sellamuthu K, Johnson RE, Prakash S, Prakash L. 2021a. A novel role of DNA polymerase λ in translesion synthesis in conjunction with DNA polymerase ζ . *Life Sci Alliance* **4**: e202000900. doi:10.26508/lsa.202000900
- Yoon JH, Johnson RE, Prakash L, Prakash S. 2021b. Implications of inhibition of Rev1 interaction with Y family DNA polymerases for cisplatin chemotherapy. *Genes Dev* **35**: 1256–1270. doi:10.1101/gad.348662.121
- Yoshimura A, Kobayashi Y, Tada S, Seki M, Enomoto T. 2014. WRNIP1 functions upstream of DNA polymerase η in the UV-induced DNA damage response. *Biochem Biophys Res Commun* **452**: 48–52. doi:10.1016/j.bbrc.2014.08.043
- You Y-H, Pfeifer GP. 2001. Similarities in sunlight-induced mutational spectra of CpG-methylated transgenes and the *p53* gene in skin cancer point to an important role of 5-methylcytosine residues in solar UV mutagenesis. *J Mol Biol* **305**: 389–399. doi:10.1006/jmbi.2000.4322
- You Y-H, Lee D-H, Yoon J-H, Nakajima S, Yasui A, Pfeifer GP. 2001. Cyclobutane pyrimidine dimers are responsible for the vast majority of mutations induced by UVB irradiation in mammalian cells. *J Biol Chem* **276**: 44688–44694. doi:10.1074/jbc.M107696200